UWB Localisation

Distributed UWB inter-ranging for MAV swarms in large GNSS-denied environments

Master Thesis

Fréderic Dupon

Delft University of Technology

TU Delft

UWB Localisation

Distributed UWB inter-ranging for MAV swarms in large GNSS-denied environments

by

Fréderic Dupon

Master Thesis to obtain the degree of Master of Science
at the Delft University of Technology,
to be defended publicly on Tuesday August 30, 2022 at 09:30 AM.

Student number:	4465040	
Exam Committee:	Dr. G.C.H.E. de Croon,	TU Delft
	Dr. J. Guo,	TU Delft
	S. U. Pfeiffer,	TU Delft
	Dr. E. J. J. Smeur,	TU Delft

1

[1] Cover Figure url: `https://www.bitcraze.io/images/frontpage/front.jpg`

TU Delft

1

Scientific Article

Distributed UWB inter-ranging for MAV swarms in large GNSS-denied environments

F.A. Dupon, S.U. Pfeiffer*, Prof. Dr. G.C.H.E. de Croon*
Delft University of Technology, Delft, The Netherlands

The use of micro air vehicles (MAV) is becoming increasingly mainstream and with them their applications have become more demanding across the board. The application of MAV's in large GNSS-denied environments often asks for a distributed and scalable localisation system with minimal reliance on static localisation hardware. In this research a distributed ultra-wideband (UWB) localisation system that takes advantage of the collaborative capabilities of a swarm of MAV's has been developed and tested in both simulation and practice. Additionally, a modular UWB simulator has been developed which enables researchers to test UWB localisation schemes for a swarm of MAV's. It has been found that when taking advantage of the UWB inter-agent ranging capabilities of a swarm of micro air vehicles, one can increase the coverage of an UWB setup in spaces with coverage-issues and conversely increase the accuracy of an existing UWB setup that has full UWB coverage.

I. Introduction

Due to recent technological advancements, unmanned aerial vehicles are becoming increasingly popular these days. They exist in all sorts of designs and shapes. Thanks to their versatility, they are being used in a wide range of applications. Unmanned aerial vehicles (UAV) are not only being used by recreational users, but also by industry and researchers. For example, they are being deployed by large multinationals to inspect wind turbine blades or oil pipelines, but they can also be found at the local park for leisure. These advancements make it possible to miniaturise the UAV's into micro air vehicles (MAV). Although they are often computationally less capable than their larger counterparts, they have the advantage that they are small, lightweight, and are often accompanied with a lower unit cost. This relatively new category of micro air vehicles gives way to a new range of applications, requiring robust and computationally lightweight solutions. Those micro air vehicles can be deployed stand-alone, but often the big advantage is that they can also be deployed in swarm configurations. In many use cases, the application of such robotic swarms can have specific advantages. A homogeneous swarm, consisting of multiple micro air vehicles performing the same action can dramatically decrease the completion time of a task, while a heterogeneous swarm, consisting of multiple unique micro air vehicles, each with their own speciality, is able to perform many different tasks at once [1].

Aside from the specific application of the micro air vehicles, they all have one thing in common: the need for a localisation system to obtain a location estimate. This is often necessary in order to perform a task accurately and autonomously. The localisation systems can be GNSS-based, but often, solutions have to be found to enable localisation in GNSS-denied environments, or environments where the reception is intermittent. For such GNSS-denied environments alternative localisation systems exist. The localisation system central to this research is the ultra-wideband (UWB) Loco Positioning System (LPS) made by Bitcraze [2]. In this paper one will investigate how one can increase the UWB localisation accuracy of a swarm of MAV's in both environments with full and intermittent UWB coverage, by making use of the collaborative capabilities of a swarm of MAV's. Please refer to Figure 1 for a depiction of a swarm of MAV's performing collaborative localisation. In the scope of this research, the industrial use case of monitoring and inspection of crops in greenhouses by a swarm of small micro air vehicles is highly relevant. It is often not possible to fit such a large space with UWB equipment enabling indoor localisation, as an UWB anchor has a limited range of around $\approx 15 - 20$ m. However, by using the transcending capabilities of a swarm of micro air vehicles it is possible to deploy an ad-hoc distributed localisation network that can cross gaps that fail to be covered by UWB anchors.

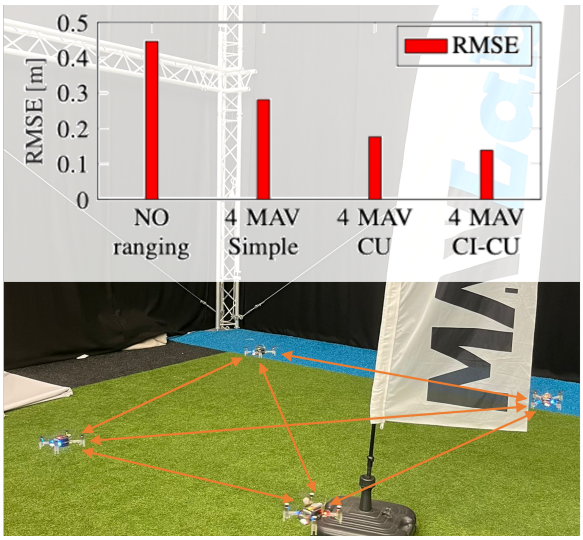

Figure 1. Swarm of 4 Crazyflies improving state-estimate by inter-agent ranging in TU Delft Cyberzoo. Exchanging more information renders lower RMSE between ground truth and state-estimate in limited-coverage environment.

*Thesis Supervisors with the Faculty of Aerospace Engineering, Delft University of Technology 2629 HS Delft, The Netherlands

The goal of this work is to implement an optimised inter-agent ranging approach for MAV swarms which enables them to be less dependent on static UWB anchors for localisation in the TU Delft Cyberzoo. The design hypothesis is that a swarm of micro air vehicles can perform inter-agent ranging with the swarm members, improving each other's state estimate, while reducing their dependence on static UWB anchors. Exploiting the inter-agent ranging capabilities of a swarm of micro air vehicles makes it possible to increase the localisation accuracy in spaces where UWB reception is intermittent, or to enable UWB localisation in large areas, without the burden of having to add numerous static anchors to the environment. Additionally, the approach presented in this paper is distributed and lightweight, such that it does not interfere with the specific task a MAV swarm member might have.

First, in Chapter II, the methodology used in this paper will be discussed. This entails fundamental UWB localisation concepts and schemes, as well as an explanation of the simulator framework developed for this research. Next, in Chapter III, the simulation tests and results will be presented, together with a thorough discussion of the results. The presented localisation schemes have been validated in practice and the results of these tests are presented in Chapter IV. Finally, this paper is concluded and proper recommendations are made. These can be found in Chapter V.

II. Methodology

In this paper, we will investigate how one can increase the UWB localisation performance of MAV's in large environments by making use of the swarming capabilities of a group of these MAV's. First, in section II.A, one will explain how localisation is achieved with UWB. After which, in Section II.B, the simulation environment used during this research will be discussed. In Section II.C, one will perform an excursion on collaborative localisation and explain how this research fits in current collaborative localisation theory. Finally, in Section II.D the UWB localisation schemes that have been investigated as part of this paper will be presented.

A. Ultra-Wideband (UWB) Localisation

Ultra-wideband is one of the most recent, accurate and promising technologies for indoor localisation [3], making use of radio technology characterised by its very large bandwidth compared to conventional narrow-band systems [4]. As stated by Alammar et al., the Federal Communications Commission (FCC) has defined UWB as a radio frequency (RF) signal covering a portion of the frequency spectrum larger than 20% of the center-carrier frequency, or having a bandwidth larger than 500 MHz [5]. Thanks to this large bandwidth of the UWB signals this technology is highly suitable for positioning systems. As ultra-wideband uses different signal types and radio spectra, it does not easily interfere with other radio frequency-based localisation systems. UWB positioning systems transmit a signal over multiple frequency bands, ranging from 3.1 to 10.6 GHz [6]. This brings advantages such as better penetration through obstacles, accurate position estimation, high-speed data transmission and low cost and low power transceiver designs [7]. In general, a data rate of about 100 Megabits per second ($Mbps$) can be achieved [3]. Thanks to the fact that UWB covers a wide portion of the frequency spectrum and transmits ultra short pulses, UWB can transmit large packets of information using very low transmission energy [5]. Also, the short pulses of the ultra-wideband localisation system are easy to filter out, meaning that it is easier to distinguish the original pulses from the pulses generated by multi-path effects and it permits determining an accurate time of flight (TOF) estimate of a burst transmission from a short-pulse transmitter [6]. This property makes that UWB becomes suitable for indoor localisation, making it possible to achieve centimetre accuracy, by exploiting the time of flight (TOF) of the signal using suitable localisation algorithms such as TOA, TDOA and others. How these are used in this paper will be explained below.

1. Time Of Arrival (TOA)

The Time Of Arrival localisation algorithm (TOA), also called Time of Flight (TOF), is based on signal propagation time between a receiver and transmitter [5]. The system is based on accurate synchronisation of the arrival time of a signal transmitted by a transmitter target to several receiver anchors [8]. The Time Of Arrival algorithm can be based on One-Way Ranging (OWR) or Two-Way Ranging (TWR). More specifically, when calculating a positioning estimate using the One-Way Ranging approach, the distance from the target to the receiver anchors is estimated, comparing the one-way arrival time of a time-stamped signal at the receiver anchor. This happens while the clocks of the anchors and target have been precisely synchronised and the location of the anchors are known. When it is not possible to accurately synchronise the receiver and transmitter's clocks, a Two-Way Ranging approach can be used. In this case, the signal travels two-ways, from transmitter to receiver and back to the transmitter. This way, the clock offset is cancelled out. Time Of Arrival is a feasible localisation algorithm, as the signal propagation speed and the time the signal takes to reach the receiving anchor is known. A Time Of Arrival measurement t_i can be seen in Equation 1, in which p is the position of the target, p_i the position of the anchor, Θ the clock offset between the anchor and target, c the speed of light and n_i the noise existing of measurement and transmission noise [9].

$$t_i = \frac{\|p - p_i\|}{c} - \Theta + n_i \tag{1}$$

The TOA algorithm was found to be an accurate solution for indoor positioning, as it is possible to filter out multi-path effects [8]. Also, by synchronised TOA measurements, localisation simplifies to the intersection of spheres, this way 3D localisation can be performed with at least 3 anchors. Please refer to Equation 2 for a depiction of how these TWR measurements are used for a localisation update with i number of anchors.

$$d_i = \sqrt{(x - x_i)^2 + (y - y_i)^2 + (z - z_i)^2} \tag{2}$$

2. Time Difference Of Arrival (TDOA)

The Time Difference Of Arrival (TDOA) localisation algorithm uses the arrival time-difference of a signal sent by a transmitter and received by three or more receivers [3]. As the time difference between arrival times of signals cancels out the offset between transmitter and receiver clock, there is no need for time-synchronisation between receiver and transmitter clock [9], as long as the receivers are synchronised. This decreases the complexity and hardware cost of the system. A Time Difference Of Arrival measurement $t_{i,j}$ can be seen in Equation 3, in which p is the position of the target, p_i and p_j are the positions of the anchors, c the speed of light, n_i and n_j the measurement and transmission noise for the respective anchors [9].

$$t_{i,j} = \frac{\|p - p_i\| - \|p - p_j\|}{c} + n_i + n_j \tag{3}$$

Position estimates are obtained by calculating the intersection of the hyperbolic curves that are obtained with each TDOA measurement [8]. In order to combine the different TDOA measurements received at each receiver anchor, the anchors have to be in contact, requiring significant bandwidth [3]. The concept of TDOA explained here involves one target transmitter and multiple receiving nodes. Please note that this concept can also be switched, in which a single target receiver measures the change in arrival time of signals transmitted by multiple anchors [3]. Please refer to Equation 4 for a depiction of how these TDOA measurements are used for a localisation measurement update with anchor i and j.

$$d_{i,j} = \sqrt{(x - x_i)^2 + (y - y_i)^2 + (z - z_i)^2} - \sqrt{(x - x_j)^2 + (y - y_j)^2 + (z - z_j)^2} \tag{4}$$

B. Simulation environment

In order to investigate the distributed UWB localisation schemes presented in this paper, the backbone of the MAV swarm simulation environment Swarmulator, developed by M. Coppola was used [10]. The original Swarmulator mainly focuses on the development of behavioural controllers for robotic swarms and therefore is lacking fundamental functionality necessary for this research. It does not include an ultra-wideband setup, no quadrotor dynamics, nor accompanying sensors and sensor fusion or state estimator filters. Therefore, it has been decided to fork Swarmulator and incorporate this extra functionality, only maintaining the animation, logger and thread management functionality of Swarmulator. Please find the additional functionalities described below and illustrated in Figure 2.

1. Trajectory generator

For every quadrotor that is spawned in the simulation environment, a predefined trajectory must be generated. The trajectory generator module can generate trajectories for the quadrotors through predefined way-points. It is based on Matlab's *waypointTrajectory* System object [11]. For every way-point the arrival time must be specified. The resulting trajectory minimises the required change in velocity and thus acceleration.

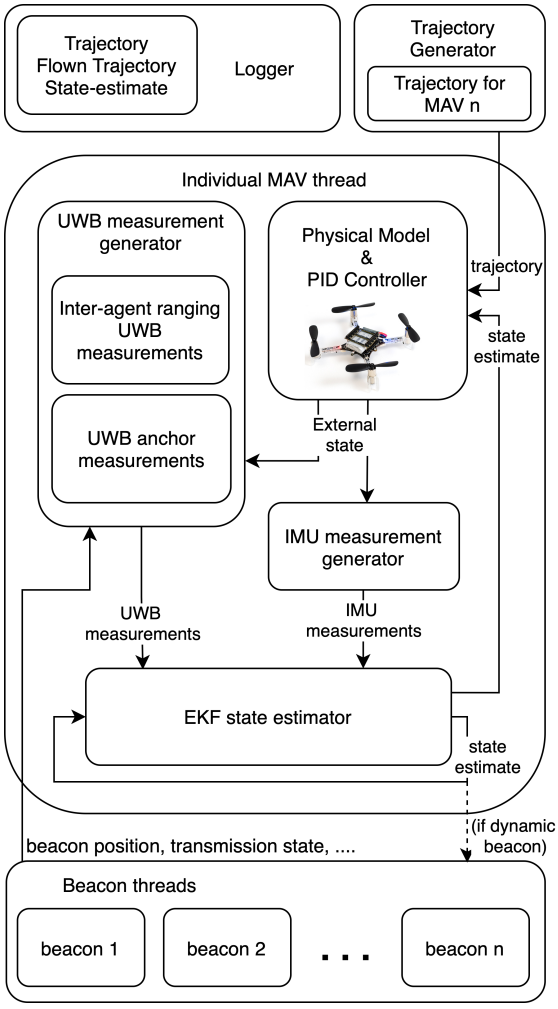

Figure 2. Simulation framework showcasing the additional functionality added to the Swarmulator environment.

This way one ensures that the generated trajectory is the least challenging for the quadrotor dynamics to attain. In the simulator and trajectory generator, the trajectory frequency can be specified as desired. By default, the trajectory is generated and read at a frequency of 100 Hz.

2. EKF sensor fusion

An Extended Kalman Filter (EKF) with constant acceleration is being used for sensor fusion and state-estimation. The filter runs at a predefined frequency of 250 Hz and can be adjusted to preference. During the prediction step an accelerometer provides acceleration measurements. The accelerometer (having zero-mean Gaussian additive noise) runs at a predefined frequency, with as default a frequency of 1000 Hz and σ of 0.01 m/s^2. Whenever an UWB measurement is available, the prediction step is followed by an UWB measurement update step. The measurement update step can perform measurement updates for TDOA or TWR UWB measurements. Additionally, it is possible to specify the maximum update frequency of the TWR and TDOA measurements. Please refer to Figure 3 for a schematic representation of the workings of this estimator.

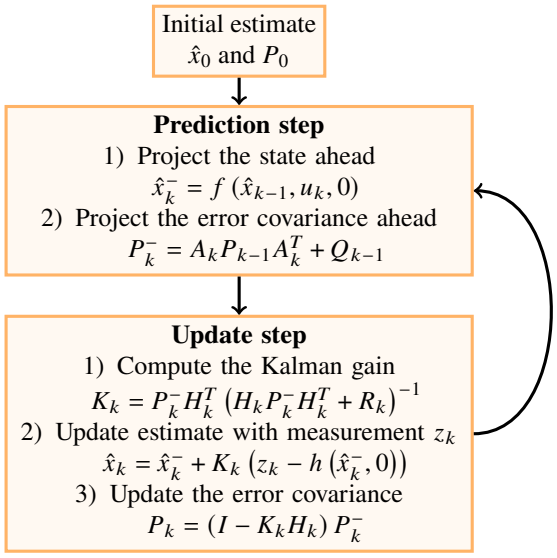

Figure 3. Illustration of the general EKF flowchart.

3. Simplified quadrotor dynamics & PID controller

The physical model of the quadrotor is implemented in similar fashion as described by Samir et al. [12] and is described by Equation 5, with x, y z being the motion along these axes as a consequence of the pitch (θ) roll (ϕ) or yaw (ψ) motion. Please note that as the simulation environment is 2D and for simplification purposes, the yaw angle and motion in z direction are set to zero. Additionally, U_1, U_2, U_3 and U_4 are depicted as the torques corresponding to the quadrotor's degrees of freedom (DOF). Zero-mean noise with σ of 0.005 is added to every torque input. The quadrotor's characteristics are modelled according to the parameters of the Crazyflie 2.0 and they can also be found in Table 1 of Appendix VI [13].

$$
\begin{aligned}
\ddot{\phi} &= \dot{\theta}\dot{\psi}\left(\frac{I_y - I_z}{I_x}\right) - \frac{J_r}{I_x}\dot{\theta}\Omega + \frac{l}{I_x}U_2 \\
\ddot{\theta} &= \dot{\phi}\dot{\psi}\left(\frac{I_z - I_x}{I_y}\right) + \frac{J_r}{I_y}\dot{\phi}\Omega + \frac{l}{I_y}U_3 \\
\ddot{\psi} &= \dot{\phi}\dot{\theta}\left(\frac{I_x - I_y}{I_z}\right) + \frac{1}{I_z}U_4 \\
\ddot{z} &= -g + (\cos\phi\cos\theta)\frac{1}{m}U_1 \\
\ddot{x} &= (\cos\phi\sin\theta\cos\psi + \sin\phi\sin\psi)\frac{1}{m}U_1 \\
\ddot{y} &= (\cos\phi\sin\theta\sin\psi - \sin\phi\cos\psi)\frac{1}{m}U_1
\end{aligned}
\tag{5}
$$

The PID controller of the quadrotor is subdivided in a linear and angular control system and steers the state-estimate towards the desired trajectory. The outer part of the PID controller controls the linear displacement in x and y direction as demanded by the specified trajectory and runs at a trajectory frequency of 100 Hz. The inner part of the PID controller controls the required rotations to achieve the desired linear displacement and runs at the simulation frequency of 1000 Hz.

4. Ultra-wideband setup

In the simulator, the basic functionality of the UWB based Loco Positioning System designed by Bitcraze has been implemented [2]. It is possible to define the location of UWB anchors —these anchors run in their own thread and transmit UWB measurements at a predefined frequency— with a specified signal length and range. One can spawn two kinds of UWB anchors in the simulation. These will be itemised below:

- *Static anchors:* It is possible to spawn static anchors in the 2D plane. These anchors have a predefined x and y location which does not change and is known by all quadrotors in the simulation.
- *Dynamic anchors:* These anchors can be seen as UWB anchors on top of *(moving)* quadrotors. This enables the quadrotor to act as tag and anchor simultaneously. Their x and y location for measurement generation correspond to the x and y true state of the quadrotor. Additionally, dynamic anchors transmit their x and y state-estimate as well as uncertainty information along with the UWB measurements. The state-estimate and measurement is used by the receiving agent for UWB localisation and can be supplemented with the received uncertainty information.

C. Swarm collaborative localisation

The goal of this research is to develop a collaborative localisation approach that makes use of UWB-inter agent ranging measurements in order to improve one's location estimate. In order to develop a suitable *distributed* collaborative localisation proposition that can be implemented on the EKF's of the individual swarm members, it is recommended to take a step back and investigate the dynamics of a swarm of inter-agent ranging agents from the centralised perspective, in which sensor fusion is performed off-board by a single entity that has access to all information of the swarm. This is important as to have a proper understanding of how inter-agent ranging can have an influence on the quadrotor's state-estimates. As a matter of fact, when a swarm of quadrotors is inter-agent ranging, their states can be expected to become correlated with respect to each other.

Let's investigate a simple case as to why the states become correlated after several inter-agent ranging measurements have taken place below, after which the equations for a centralised EKF of n robots will be presented. This is the ideal-case centralised scenario, which takes into account the implications of inter-agent ranging measurements on the cross-correlation between the states of the quadrotors. The centralised approach does not have communication or computational constraints that come with a distributed approach and is therefore a good basis for the derivation of a distributed scheme. Once the centralised EKF is derived, it is possible to make a proposition to how one can design a distributed approach and how this distributed approach is compromised as compared to the centralised EKF. These compromises arise from the inherent characteristics of a swarm of micro MAV's, that generally come with communication and computational power constraints. The distributed propositions that will be tested in this paper will be discussed in Section II.D.

1. Simple inter-agent ranging example

The example that will be presented in this paper is extracted from the example discussed by I. Roumeliotis et al. on their paper on distributed collective localisation [14]. Let's assume two robots (A & B) having on-board sensors to construct their own state-estimate and the additional capability to perform inter-agent ranging with respect to each other. Every robot has its own independent uncertainty estimate related to it's own position. Under the assumption that the estimate of A and B are independent, the additional uncertainty for robot A due to an inter-agent ranging measurement between agent A and B can be depicted by Equation 6, with $P_{A(m)}$ being the additional uncertainty due to the measurement, $P_{\Delta A,B}$ corresponding to R, being the measurement noise of the inter-agent ranging measurement and $P_{B(-)}$ being the uncertainty estimate of agent B at the time of the measurement.

$$P_{A(m)} = P_{\Delta A,B} + P_{B(-)} = R + P_{B(-)} \tag{6}$$

After agent A performs an inter-agent ranging measurement with respect to agent B, agent A can update its uncertainty estimate by merging the uncertainty corresponding to the inter-agent ranging measurement with it's own estimate. This is depicted by Equation 7. Rewriting this relationship, one can see that the estimated location of robot A becomes the weighted average of robot A's estimated position and uncertainty, together with the estimated position and uncertainty acquired from the inter-agent ranging measurement. This is also wat happens when performing a simple measurement update in an EKF or KF. The updated estimate can be seen in equation 8, with X_A being the self-estimated location of robot A and $X_A(m)$ being the estimated location of robot A due to the ranging measurement.

$$P_A^{-1} = P_{A(-)}^{-1} + P_{A(m)}^{-1} \tag{7}$$

$$P_{A(+)}^{-1} X_A(+) = P_{A(-)}^{-1} X_A(-) + P_{A(m)}^{-1} X_A(m) \tag{8}$$

Please note that above relations are only valid under the assumption that the state of agent A and B are independent. After the first ranging measurement, the states of the agents become correlated. Assuming independence and thus not taking into account cross-covariances between the agent's states will result in under-estimation of the agent's uncertainty. This also shows the importance of an optimised inter-agent ranging approach. Not including uncertainty information can not only lead to a grave measurement error, but also to an exponential decrease in uncertainty, which can in turn lead to an inconsistent outcome of the state-estimator [14].

Take once again the example explained by I. Roumeliotis et al. [14]. We have two agents A and B, that have both an initial uncertainty P_A and P_B of value 4 each. Lets assume they inter-agent range once. Their updated uncertainty becomes P_A and P_B of value 2. Now assume agent A and B each move again, which adds an uncertainty of 8 to each of the agent's uncertainty values. When the quadrotors range again under the assumption that their state estimates are still independent, their updated uncertainty information is $10/2 = 5$. However, this is an under-estimation. After the first inter-agent ranging measurement, the state-estimates of agent A and B have become correlated. The uncertainty corresponds to a value of $2 + 4 = 6$, which takes into account the independent parts of information [14].

2. Centralised EKF excursion for n inter-agent ranging quadrotors

A suitable way of investigating how the states of quadrotors are evolving while inter-agent ranging is by deriving the equations for a centralised EKF of n quadrotors. Let's assume agent 1 is inter-agent ranging towards agent 2. For a schematic representation of the workings of an EKF, please refer to Figure 3. The combined state-vector of all quadrotors in the swarm is represented by matrix $\hat{x}_n$ and is projected ahead by every quadrotor individually. It is assumed that the quadrotors move independently according to their own state propagation functions. Please refer to equations 9 and 10 for these first steps.

$$\hat{x}_{k,n}^{-} = f\left(\hat{x}_{k-1,n}, u_{k,n}, 0\right) \tag{9}$$

with

$$\hat{x_n} = \begin{bmatrix} \hat{x_1} & \hat{x_2} & \dots & \hat{x_{n-1}} & \hat{x_n} \end{bmatrix}^T \tag{10}$$

After propagating the state ahead, one can do the same for the error covariance of each quadrotor. $P_{n,n}$ denotes the error covariance matrices for every agent of the swarm, including their cross-covariances. Please note that after the first inter-agent ranging measurement update step, cross-correlations are introduced. Before the first measurement update step, cross-correlations (off-diagonal error-covariance elements) are zero. Please find the final part of the EKF prediction step in equation 11 to 15.

$$P_k^{-} = A_k P_{k-1} A_k^T + Q_{k-1} \tag{11}$$

with

$$A_k = \begin{bmatrix} A_{k,1} & 0 & \dots & 0 & 0 \\ 0 & A_{k,2} & \dots & 0 & 0 \\ \vdots & \vdots & \vdots & \vdots & \vdots \\ 0 & 0 & \dots & A_{k,n-1} & 0 \\ 0 & 0 & \dots & 0 & A_{k,n} \end{bmatrix} \tag{12}$$

$$P_{k-1} = \begin{bmatrix} P_{k-1,1,1} & P_{k-1,1,2} & \dots & P_{k-1,1,n-1} & P_{k-1,1,n} \\ P_{k-1,2,1} & P_{k-1,2,2} & \dots & P_{k-1,2,n-1} & P_{k-1,2,n} \\ \vdots & \vdots & \vdots & \vdots & \vdots \\ P_{k-1,n-1,1} & P_{k-1,n-1,2} & \dots & P_{k-1,n-1,n-1} & P_{k-1,n-1,n} \\ P_{k-1,n,1} & P_{k-1,n,2} & \dots & P_{k-1,n,n-1} & P_{k-1,n,n} \end{bmatrix} \tag{13}$$

$$Q_{k-1} = \begin{bmatrix} Q_{k-1,1} & 0 & \dots & 0 & 0 \\ 0 & Q_{k-1,2} & \dots & 0 & 0 \\ \vdots & \vdots & \vdots & \vdots & \vdots \\ 0 & 0 & \dots & Q_{k-1,n-1} & 0 \\ 0 & 0 & \dots & 0 & Q_{k-1,n} \end{bmatrix} \tag{14}$$

resulting in

$$P_k^- = \begin{bmatrix} A_{1,k} \cdot P_{k-1,1,1} \cdot A_{1,k}^T + Q_{k-1,1} & A_{1,k} \cdot P_{k-1,1,2} \cdot A_{2,k}^T & \dots & A_{1,k} \cdot P_{k-1,1,n-1} \cdot A_{n-1,k}^T & A_{1,k} \cdot P_{k-1,1,n} \cdot A_{n,k}^T \\ A_{2,k} \cdot P_{k-1,2,1} \cdot A_{1,k}^T & A_{2,k} \cdot P_{k-1,2,2} \cdot A_{2,k}^T + Q_{k-1,2} \dots & & A_{2,k} \cdot P_{k-1,2,n-1} \cdot A_{n-1,k}^T & A_{2,k} \cdot P_{k-1,2,n} \cdot A_{n,k}^T \\ \vdots & \vdots & \vdots & \vdots & \vdots \\ A_{n-1,k} \cdot P_{k-1,n-1,1} \cdot A_{1,k}^T & A_{n-1,k} \cdot P_{k-1,n-1,2} \cdot A_{2,k}^T & \dots A_{n-1,k} \cdot P_{k-1,n-1,n-1} \cdot A_{n-1,k}^T + Q_{k-1,n-1} & & A_{n-1,k} \cdot P_{k-1,n-1,n} \cdot A_{n,k}^T \\ A_{n,k} \cdot P_{k-1,n,1} \cdot A_{1,k}^T & A_{n,k} \cdot P_{k-1,n,2} \cdot A_{2,k}^T & \dots & A_{n,k} \cdot P_{k-1,n,n-1} \cdot A_{n-1,k}^T & A_{n,k} \cdot P_{k-1,n,n} \cdot A_{n,k}^T + Q_{k-1,n} \end{bmatrix} \quad (15)$$

One can see that during a prediction step of a swarm of MAV's, one does not only has to propagate the agent's individual covariance matrices, but also the cross-covariance matrices of all the quadrotors in the swarm. This comes with a higher computational load than when an an agent just has to propagate its own auto-covariance. In absence of this constraint, it is possible to convert this centralised EKF in a distributed EKF by distributing all the equations of the EKF under the agents of the swarm. However, this comes with a high communication load, which is most often not available in a fully decentralised swarm. Additionally, it is often not possible for a scalable distributed swarm to communicate the calculated cross-covariance matrices with all agents of the swarm. Apart from the computational and communication constraints, it is also difficult to make this approach scalable for a dynamically varying number of swarm members.

In order to figure out how the uncertainty of a ranging-agent can be included in our decentralised inter-agent ranging schemes, the second part of the centralised EKF excursion will be performed as well. Here, the centralised EKF measurement update equations will be derived for an inter-agent measurement update between agent 1 and 2. Once again, it is assumed that some inter-agent ranging updates have taken place already, rendering non-zero cross-covariance terms. First, the Kalman gain for an inter-agent ranging measurement between agent 1 and 2 must be computed and is depicted in Equation 16 to 18.

$$K_k = P_k^- H_k^T \left(H_k P_k^- H_k^T + R_k \right)^{-1} \quad (16)$$

$$K_k = \begin{bmatrix} (P_{k,1,2}^- - P_{k,1,1}^- H_{k,1,2}^T) S_{k,1,2}^- \\ (P_{k,2,2}^- - P_{k,2,1}^- H_{k,1,2}^T) S_{k,1,2}^- \\ (P_{k,3,2}^- - P_{k,3,1}^- H_{k,1,2}^T) S_{k,1,2}^- \\ \vdots \\ (P_{k,n-1,2}^- - P_{k,n-1,1}^- H_{k,1,2}^T) S_{k,1,2}^- \\ (P_{k,n,2}^- - P_{k,n,1}^- H_{k,1,2}^T) S_{k,1,2}^- \end{bmatrix} \quad (17)$$

with

$$S_{k,1,2}^- = H_{k,1,2} P_{k,1,1}^- H_{k,1,2}^T - P_{k,2,1}^- H_{k,1,2}^T - P_{k,1,2}^- H_{k,1,2} + P_{k,2,2} + R_k \quad (18)$$

Finally, after calculation of the Kalman gain, the state of the inter-agent ranging quadrotors is updated, after which the EKF update step is finalised by updating the cross- and auto-covariances as well. For a depiction of these steps, please refer to Figure 3. Similar to the prediction step of the centralised EKF, the update equations of the centralised EKF can be distributed over all quadrotors in the swarm as well. However, this is challenging the same computational and communication constraints as with distributing the prediction step equations. Another interesting note is the fact that not only the quadrotors taking part in the inter-agent ranging measurement are affected by the ranging measurement. As a matter of fact, due to the measurement update between agent 1 & 2, the other agents experience an information change as well, for which one has to compensate. One can see the cross-covariances as how much information is shared between the agents [14][15]. Therefore if agents undergo a change in information due to inter-agent ranging, every agent in the swarm can update their view on this information. This brings along an extra measurement update scheduling challenge. In turn, one can also see that in case all agents share the same information —cross-covariances— the update reduces to only the ranging agent. How this centralised EKF will be simplified in a distributed approach will be explained in the next section.

D. Distributed collaborative localisation for swarming

For UWB localisation of a single MAV in environments where UWB anchor coverage or accuracy is not an issue, one can make use of readily available positioning algorithms based on TWR or TDOA as discussed in Section II.A. As a matter of fact, one should not only be able to take advantage of the information provided by the static UWB anchors (TDOA), but also of the information provided by other agents in the swarm (TWR). The *hybrid TDOA-TWR* localisation schemes proposed here make it possible for an agent to perform TDOA with static anchors and TWR between dynamic anchors (agents) when in range. As explained in Section II.C, exchanging ranging information between quadrotors can result in correlated states and often comes with a high communication and computational burden. Therefore, the schemes presented in this section will undergo some crucial simplifications that allows them to become lightweight and distributed.

First, in Subsection II.D.1, the implementation of the *simple hybrid TDOA-TWR* distributed localisation scheme will be discussed. This is the most simplified approach, in which the quadrotor does not take into account uncertainty information of ranging quadrotors. Next, in Subsection II.D.2, one will propose a *covariance updated (CU) hybrid TDOA-TWR* localisation scheme, which aims at counteracting ranging uncertainty by taking into account the auto-covariance of the ranging MAV by augmenting the ranging measurement noise. Finally, in Subsection II.D.3, one will discuss the *Covariance intersection covariance updated (CI-CU) Hybrid TDOA-TWR* scheme, which does not only takes into account the auto-covariance values of the ranging quad-rotors by augmenting the measurement noise, but also attempts at conservatively fusing the measurement estimate under unknown correlation.

1. Simple Hybrid TDOA-TWR for swarming
In the simple inter-agent ranging approach the MAV's are performing TDOA with static anchors and TWR in between swarm members. When performing TWR, the TWR measurement —which is a proxy for the distance between two agents— is communicated, together with the state-estimate of the transmitting quadrotor. This means that during an inter-agent ranging measurement towards a quadrotor, no extra uncertainty information is exchanged, except for the quadrotor's state-estimate. It is essential that the state-estimate is communicated, as this is an estimate for the anchor's position at the time of the measurement and the only position metric that is known by the quadrotor's in the swarm. When the EKF in the ranging quadrotor receives a ranging measurement, the associated measurement noise is only based on the noise of the ranging measurement and no noise correction is made for the uncertainty of the quadrotor; the error between the quadrotor's state and state-estimate. For a graphical representation of this method, please refer to Figure 4. This method is based on some simplifications and assumptions, which are itemised below:

- It is assumed that the position of the dynamic anchor is the state-estimate of the ranging quadrotor. This means that the error between the ranging quadrotor's state and state-estimate will be propagated through the TWR measurement if no correction for this uncertainty is made.
- It is assumed that the states of all quadrotors are independent (cross-correlations $P_{k,i,j}$ are zero with $i, j \epsilon \{1, 2, \ldots, n\} \wedge i \neq j$) and that they remain independent after inter-agent raging has taken place.
- In order to limit communication, no auto-covariance metrics are communicated in between the quadrotors. Instead, a ranging quadrotor only receives the ranging TWR measurement and a state-estimate.

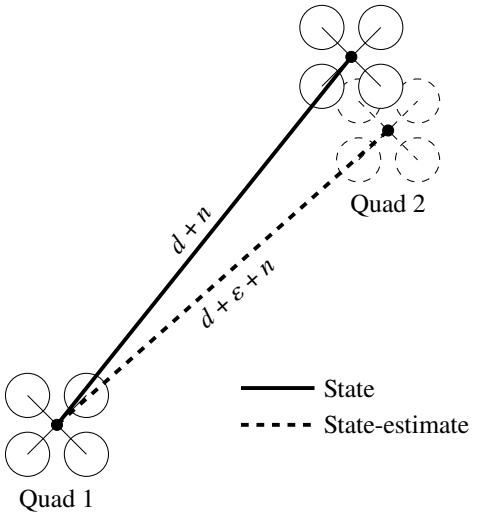

Figure 4. Quad 1 simple inter-agent ranging with Quad 2.

Above assumptions enable the centralised EKF to become a fully distributed one. Implementing above assumptions in the EKF of an individual quadrotor, one can rewrite Equation 16 and find the associated measurement update equations for an inter-agent ranging measurement between quadrotor 1 and 2 of a swarm of n quadrotors. These are described in Equation 19 to 21. One can see that in this decentralised implementation, only the ranging quadrotor is involved in the measurement update, as full independence between the quadrotors states is assumed.

$$K_k = P^-_{k,1,1} H^T_{k,1,2} (H_{k,1,2} P^-_{k,1,1} H^T_{k,1,2} + R_k)^{-1} \tag{19}$$

$$\hat{x}_1 = \hat{x}_1 + K_k (z - z_m) \tag{20}$$

$$P_{k,1,1} = (I - K_k H_{k,1,2}) P^-_{k,1,1} \tag{21}$$

The simple inter-agent ranging approach has both it's upsides and downsides. On the one hand it is computationally lightweight and does not require extensive inter-swarm communication, while on the other hand the simplifications made have the potential to gravely influence the performance of this localisation scheme. The larger the error between the MAV's state and state-estimate, the larger the inter-agent ranging error. Not correcting for this error can affect the performance of this scheme. One can reason that the receiving quadrotor will assume a measurement noise that is too low to compensate for the error between state and state-estimate of the ranging quadrotor, shifting it's own state estimate towards the erroneous state-estimate measurement of the ranging quadrotor. Please refer to Figure 4 for a schematic representation of such an inter-agent ranging measurement and how the state/state-estimate delta can cause erroneous measurements. Additionally, when no correction is made for the auto- and cross-correlations of the inter-agent ranging quadrotors of the swarm, the agents of the swarm will tend to consistently underestimate their own state-covariance. Underestimating this covariance can render the quadrotor's filter inconsistent, as explained in Section II.C. The performance of this ranging scheme will be evaluated in Chapter III and IV.

2. Covariance updated Hybrid TDOA-TWR for swarming
As explained in the previous section, the simple *Hybrid TDOA-TWR for swarming* scheme is a highly simplified inter-agent ranging scheme which is prone to errors. These errors occur as no correction is made for the fact that one is ranging towards an uncertain source. Therefore, we propose an improved covariance updated (CU) *Hybrid TDOA-TWR for swarming* scheme, which takes into account the uncertainty measures of the ranging quadrotor in the form of an augmented measurement noise that takes into account auto-covariance measures. Once again, this localisation scheme is based on some assumptions and simplifications, which are itemised below:

- It is assumed that the position of the dynamic anchor is the state-estimate of the ranging quadrotor. This means that the error between the ranging quadrotor's state and state-estimate will be propagated through the TWR measurement if no correction for this uncertainty is made.
- It is assumed that the states of all quadrotors are independent (cross-correlations $P_{k,i,j}$ are zero with $i, j \epsilon \{1, 2, \ldots, n\} \wedge i \neq j$) and that they remain independent after inter-agent ranging has taken place.

- It is assumed that the filter on the ranging quadrotor is consistent. This means that one assumes zero-mean estimation errors, together with a covariance matrix of the output that is smaller or equal to the calculated covariance matrix [16].

As explained in Section II.B, every quadrotor in the swarm runs an EKF for state-estimation. The EKF of the MAV consists of a prediction step and an update step. For clarification, the steps of an EKF for state-estimation are presented in Figure 3. During every prediction and update step, the covariance estimate P_k of the quadrotor's state is updated. The covariance matrix $P_{k,t}$ of an agent at a time t is a proxy for the quadrotor's confidence in it's own state-estimate. As a matter of fact, the covariance matrix is also often called the error covariance matrix, as it describes the predicted error between the quadrotor's state and predicted state-estimate. An example of how such a covariance matrix evolves in absence of measurement updates is illustrated in Figure 5. There one can see an evaluation of the covariance error ellipse in absence of measurement updates for a simulation time of 26 seconds. One can see that the state is drifting away from it's state-estimate and desired trajectory, and this growing uncertainty can also be seen in the growing error ellipse.

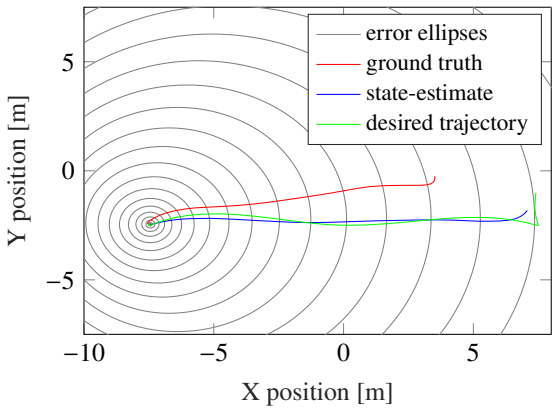

Figure 5. Growing covariance error ellipse for a drifting MAV.

Upon performing a TWR measurement update, the TWR measurement receives a weight corresponding to the Kalman Gain K. In turn, this Kalman gain is influenced by the measurement noise R, that is associated with the received measurement. In the simple *Hybrid TDOA-TWR for swarming* approach, this measurement noise was solely based on the noise associated with the TWR measurement and no extra noise factor corresponding to the uncertainty of the quadrotor about it's state was included. The CU *Hybrid TDOA-TWR for swarming* approach aims at augmenting the measurement noise to include the uncertainty modelled by the covariance error matrix. Implementing above assumptions in the EKF of an individual quadrotor, one can once again rewrite Equation 16 and find the associated measurement update equations for an inter-agent ranging measurement between quadrotor 1 and 2 of a swarm of n quadrotors.

$$K_k = P^-_{k,1,1} H^T_{k,1,2} (H_{k,1,2} P^-_{k,1,1} H^T_{k,1,2} + P_{k,2,2} + R_k)^{-1} \quad (22)$$

$$\hat{x}_1 = \hat{x}_1 + K_k (z - z_m) \quad (23)$$

$$P_{k,1,1} = (I - K_k H_{k,1,2}) P^-_{k,1,1} \quad (24)$$

Rewriting Equation 22, the relation for $R_{TWR-COV}$ can be deducted as depicted in Equation 25, with $R_{TWR-COV}$ being the updated noise variance.

$$R_{TWR-COV} = P_{k,2,2} + R_k \quad (25)$$

Now, in order to reduce the covariance matrix to a scalar, enabling the quadrotor to perform a scalar measurement update, one can take into account the covariance $P_{k,2,2}$ of the ranging quadrotor in the direction of the measurement update. This has the advantage that the covariance of the residual becomes a scalar, which is easily invertible in calculation of the Kalman gain. Mathematically, the variance of an error ellipse under an angle can be calculated with the transformation as shown in Equation 26.

$$S_{dd} = S_{xx} \cos^2\theta + 2S_{yx} \cos\theta \sin\theta + S_{yy} \sin^2\theta \quad (26)$$

With S_{xx}, S_{xy} and S_{yy} being the variances and covariances of the error ellipse over their respective axis and θ being the angle between the quadrotor's states in the xy plane. For a graphical representation, please refer to Figure 6. Please note that as only the state-estimates are known, the angle between the state-estimates is used for this calculation, which can be a source of error. Finally, the variance of the measurement noise corresponding to a TWR inter-agent ranging measurement taking into account the uncertainty associated by the MAV's error-ellipse in the direction of the ranging measurement is illustrated in Equation 27. For a visual representation of how the covariance error ellipse can be used to update the measurement noise of an inter-agent ranging measurement, please refer to Figure 6.

$$R_{TWR-COV} = \sigma^2_{TWR} + S_{dd} \quad (27)$$

With $R_{TWR-COV}$ being the updated noise variance, σ^2_{TWR} being the original TWR noise variance and S_{dd} being the variance of the quadrotor's covariance error ellipse in the direction of the measurement.

Additionally, the transformation and assumptions made in Equation 26 and 27 have been validated by means of several Monte Carlo simulations. A quadrotor has been simulated to fly a rectangular trajectory as presented in Section III.A and it's corresponding state, state-estimate and error-covariance matrix values have been logged for a duration of 110 seconds. For every logged data-point of the simulation, 1000 pseudo TWR measurements have been generated, polled from the plane of the covariance error-ellipse. The variance of this data-set corresponds to the simulated measurement noise variance during 120 seconds of simulation. Subsequently, the measurement noise variance has also been calculated according to the transformation presented in Equation 26 and 27. With as angle θ, the

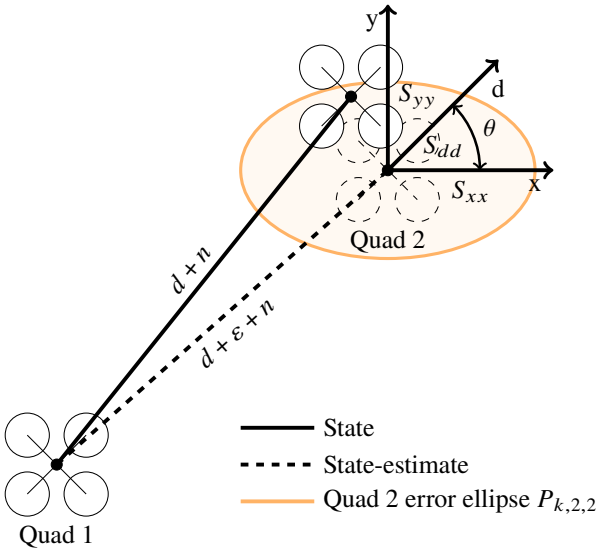

Figure 6. Quad 1 covariance updated (CU) inter-agent ranging towards Quad 2.

angle between the state-estimates. In Figure 7, one can see that the variance calculated with the relation presented in Equation 26 and 27 accurately approximates the simulated variance and therefore validating our approach.

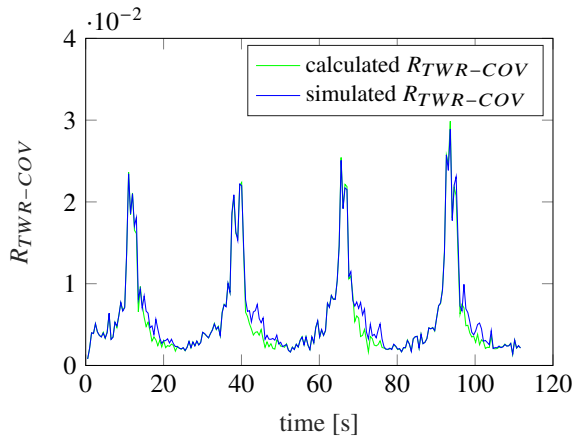

Figure 7. Calculation and simulation of $R_{TWR-COV}$ for validation purposes.

Please note that the differences between the simulated and calculated variance can be attributed to the fact that the state-estimate has been used to calculate the angle between the quadrotors, instead of the state. Therefore, as long as the MAV's state-estimate approximates the state, one can validate the approach under the assumptions made at the beginning of this section. Additionally, one has to keep in mind that the true mean of the Gaussian generated by the EKF does not always follow the approximated mean, which is also a factor that can affect the performance of this covariance updated approach. The EKF linearises the system dynamics, while these are inherently non-linear. Because of the linearisation around a single point, the covariance matrix is an approximate Gaussian ellipse, in which the true mean does not always follow the approximated mean. One could obtain a better approximation of the Gaussian ellipse by means of the Unscented Kalman Filter (UKF), in which one calculates not one, but multiple sigma-points which are used for the Gaussian transformation, rendering a better approximated Gaussian and a better approximated mean. Please refer to Figure 8 for a schematic representation of this deficiency. Additionally, as this approach does not take into account, nor compensates for the exclusion of cross-covariance factors between the quadrotors, there is the risk that the EKF becomes inconsistent after which the EKF underestimates the true covariance error ellipse, reducing the performance of this localisation scheme. In Chapter III and IV, this presented localisation scheme will be evaluated and one will investigate whether this scheme does render favourable results, regardless of the simplifications and assumptions applied in this scheme.

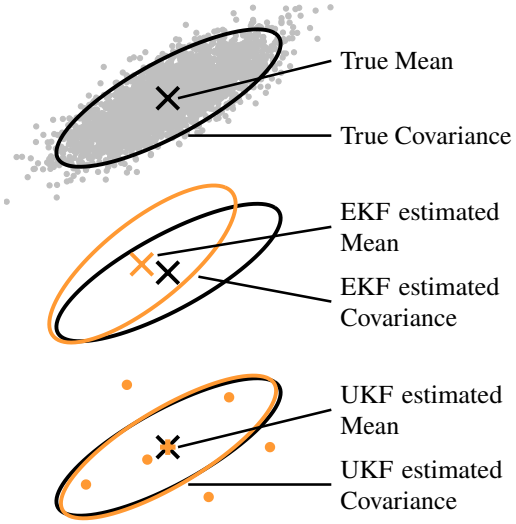

Figure 8. Error covariance ellipses for EKF & UKF.

3. Covariance Intersection noise augmentation for distributed swarming

As explained in Section II.C, the ideal case scenario for inter-agent ranging of a swarm of quadrotors involves a centralised EKF, or a distrubuted EKF with extensive communication and computational resources. These scenarios enable optimal fusion of uncertainty information, taking into account interdependencies between the states of the swarm members. However, in a decentralised swarm consisting of micro MAV's, extensive communication and computational resources are not available. In order to overcome this burden, two simplified inter-agent ranging schemes have been presented in Section II.D.1 and II.D.2. Both of these schemes come with the assumption that the states of the quadrotors in the swarm are independent and they remain independent after inter-agent ranging has taken place. Additionally, it has been shown in Section II.C that not taking into account the dependent part of information during an inter-agent ranging update has the potential to consistently underestimate the error-covariance of the ranging agent, rendering

the state-estimation filter inconsistent over time.

The author proposes to augment the measurement noise and distance measurement of the EKF measurement update step of the *CU Hybrid TDOA-TWR* localisation scheme with the Covariance Intersection (CI) method. The CI method aughts to fuse two estimates that have unknown cross-correlation in a conservative manner, taking into account an estimated cross-covariance of the two fused estimates. This is done by calculating a conservative covariance ellipse that encloses the intersection region of the two estimates, regardless of the cross-covariance between those estimates [17][18][19]. The CI method is illustrated in Equation 28. Additionally, ω must be chosen to optimise a selected criterion rendering conservative cross-covariance estmiates (e.g. trace of P_{CI}). As this decentralised localisation system aims at being lightweight and computationally efficient, an approximated optimal ω is calculated, according to Equation 29 and as discussed by [20][21].

$$\begin{aligned} P_{CI}^{-1} &= \omega P_1^{-1} + (1-\omega) P_2^{-1} \\ P_{CI}^{-1}\hat{X}_{CI} &= \omega P_1^{-1}\hat{X}_1 + (1-\omega) P_2^{-1}\hat{X}_2 \end{aligned} \tag{28}$$

$$\omega = \frac{\left|P_1^{-1} + P_2^{-1}\right| - \left|P_2^{-1}\right| + \left|P_1^{-1}\right|}{2\left|P_1^{-1} + P_2^{-1}\right|} \tag{29}$$

Instead of performing the covariance intersection method on the full state-estimates of the quadrotors, it has been decided to augment the ranging distance measurement and associated measurement noise with the CI method in one dimension; the direction of the ranging measurement. This is done by transforming the covariance matrices in the direction of the measurement. The CI method for an agent i receiving a measurement from agent j is described below.

Agent i receives an inter-agent ranging measurement d from agent j, together with agent j's estimated position $\hat{x}_j$ and covariance block p_j. The covariance is transformed in the direction of the ranging measurement and added to the ranging measurement noise. This is the first estimate $\hat{X}_1$ and associated covariance P_1^{-1} of the ranging measurement. Next, the second estimate $\hat{X}_2$ is constructed from estimated quantities, being the estimated position $\hat{x}$ of agent j and agent i. The associated covariance of this estimate consists of the measurement noise of the ranging measurement with the transformed covariance blocks of agent i and j added to it. This is the second estimate. Finally, equation 28 and 29 are applied and an updated ranging distance and measurement noise are obtained. This measurement is then processed by the normal EKF measurement update equations.

This variation on the CI method attempts to mitigate some inconsistency problems that can arise from underestimating the variance associated with a ranging measurement update. One has to be aware that manipulating the measurement and measurement noise increases the computational requirements of the localisation schemes. However, as this method applies CI in one dimension, matrix inversions reduce to scalar division, which is relatively computationally lightweight. How this *CI-CU Hybrid TDOA-TWR* scheme performs in comparison to the other schemes will be discussed in Chapter III and IV.

III. Simulation Results & Discussion

In this section, the performance of the *simple*, *CU* and *CI-CU Hybrid TDOA-TWR* localisation schemes will be evaluated by means of a simulation. The simulations are generated with the simulator model described in Section II.B and the applied algorithms are implemented as explained in Section II.D. First, in Section III.A the simulated test-setup and simulation scenarios will be discussed, after which in Section III.B and III.C the results of simulated tests with full anchor coverage and limited anchor coverage respectively will be discussed. Additionally, in Section III.D, an exploration on the EKF consistency will be performed involving how the presented localisation schemes affect this performance metric.

A. Simulated test-setup

In order to evaluate the UWB positioning schemes presented in this paper, a 2D test-setup has been developed and implemented in the modified Swarmulator simulator. For every simulated test-case in this paper, the same base test-setup has been used. This decision has been made in order to ensure uniformity and comparability between the tests. During the tests, the quadrotors will fly a trajectory consisting of an approximated rectangle of 15×5 meters in anti-clockwise direction. This trajectory has been optimised such that it minimises changes in velocity, making it less challenging for the MAV's dynamics to attain. The trajectory will be flown once by each MAV, for a total of 65 seconds. In case multiple MAV's are spawned in the simulation, all of the MAV's are flying the same trajectory and are equally distributed along the trajectory.

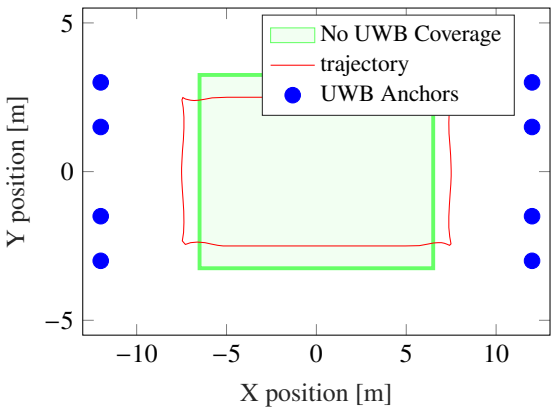

Figure 9. Visualisation of the simulated test-setup.

A total of 8 static UWB anchors have been placed in the test-environment. Their locations are tabulated in Table 2 of the Appendix. It is possible to vary the frequency at which the anchors transmit UWB packages, this to ensure the desired UWB measurement update frequency can be attained. In turn, one can change the desired UWB measurement update rate for inter-agent ranging TWR measurements and for TDOA measurements with static UWB anchors. One can also spawn dynamic anchors for every agent in the simulation, or specify a maximum range for UWB anchors. For more information regarding the simulator, please refer to Section II.B. For a depiction of the simulation test-setup, please refer to Figure 9.

All the tests performed in this section will be making use of the same base parameters. It has been decided to run the simulation at the default frequency of 1000 Hz, with an EKF frequency of 250 Hz. Additionally, the TDOA measurement update frequency has been set to 50 Hz. This has been validated by observing the achieved TDOA package update rate of a Crazyflie in the UWB setup at the TU Delft Cyberzoo [22]. Bitcraze has specified that the best TDOA performance for a scalable setup is achieved by limiting the total UWB packages to 400 packages/s. This to avoid collision between packages. Therefore, with 8 static anchors in the test-setup, it has been decided to limit the transmission frequency of the static UWB anchors to 50 Hz per anchor. Similarly, when quadrotors are TWR inter-agent ranging, the maximum of aired packages is also limited to 400 packages/s, limiting the dynamic anchors' transmission frequency to $400/n$, with n being the number of inter-agent ranging agents. In practice, TDOA and TWR can be performed on different UWB channels, decreasing the risk of collision.

The TDOA and TWR measurements are being generated by calculating the distance between the states of the agent and overlaying this measurement with zero-mean Gaussian noise. A TDOA measurement is calculated with a Gaussian noise profile with σ of 0.22 m and a TWR measurement with a noise profile with σ of 0.16 m. This has also been validated by static test data of the Loco Positioning System anchors and nodes [2][22]. These values have also been adapted in the quadrotor's EKF as fixed measurement noise values. This decision has been made as one would like to evaluate the effects of optimised inter-agent ranging schemes, while simultaneously ruling out errors induced by a sub-optimal choice of measurement noise. For future research, the dynamic calculation of measurement noise is implemented as well in the Simulator.

It has been decided to evaluate the performance of the presented localisation schemes by varying the number of inter-agent ranging quadrotors between $1-8$, as well as by varying the inter-agent ranging frequency in 20 steps between 2 and 20 Hz, with the maximum of 20 Hz being double the TWR inter-agent ranging frequency that can be attained with the Crazyflie 2.1 hardware and inter-agent ranging Loco positioning decks [2]. The data-points with a single quadrotor $n = 1$ correspond to a non-cooperative EKF. In order to be able to infer conclusions from this simulation, a total of 30 simulations have been performed for every data-point in the subsequent evaluations. This has been made possible by running 30 forked Swarmulator simulations in parallel on a Google Cloud console instance, running a general purpose E2 CPU, with 8 vCPU's and 32GB of memory. Generation of a single surface plot consisting of 120 data-points, entails a total of 4800 simulations and takes about 14 hours and 40 minutes to complete. For a more thorough discussion of the retrieved data please refer to the sections below.

In order to properly evaluate the performance of the inter-agent ranging schemes, it has been decided to test all schemes for a full-coverage test-case and a limited coverage test case. For the full-coverage test scheme the quadrotors have connection to the UWB anchors at all times. During the limited-coverage test case, the test-setup is augmented with a zone in which there is no connection to the static UWB anchors. In that zone, quadrotors have to rely on inter-agent ranging with other swarm agents in order to correct for their IMU drift and achieve accurate positioning. Please refer to Figure 9 for a representation of this limited coverage setup. For a discussion of the results of the full-coverage test and limited-coverage test-case please refer to Subsection III.B and III.C respectively.

B. Inter-agent ranging full-coverage test results

The first tests that have been performed are simulated full-coverage tests. These tests consist of a varying number of quadrotors flying in the simulated test-setup as described in Section III.A and illustrated in Figure 9. Please note as these are the full-coverage tests, the zone without UWB coverage has been disabled for these tests. All test results presented in this section have been performed for the *simple*, *CU* as well as the *CI-CU Hybrid TDOA-TWR* inter-agent ranging schemes.

For the full-coverage test-case it has been decided to not put limits on the UWB beacon range. Bitcraze has specified that the maximum range of UWB anchors is about $\approx 15-20$ m and this value fluctuates dependent on the specific hardware setup [2]. Additionally, as the intention of these simulated tests is to objectively quantify the performance of the proposed inter-agent ranging schemes, it has been decided not to limit the measurement range between the inter-agent ranging agents. Surface plots with the results of the *simple*, *CU*, as well as the *CU-CI Hybrid TDOA-TWR* inter-agent ranging scheme for the full-coverage test-case can be found in Figure 20, 21 and 22 of Appendix VI respectively.

1. Varying number of quadrotors

It is possible to slice the surface plots resulting from this test-case along the inter-agent ranging frequency axis. This way one can take a look at the the inter-agent ranging performance when varying the number of quadrotors while keeping the inter-agent ranging frequency fixed. Slices of the surface plot with an inter-agent ranging frequency of respectively 2, 10 and 20 Hz can be seen in Figure 10.

One can see that when increasing the number of quadrotors flying the trajectory, the localisation error is decreasing given that the inter-agent ranging frequency is kept high enough. As a matter of fact, when varying the number of quadrotors between $1-8$, one can observe for the *simple* scheme a maximum localisation improvement of 23.12%, for the *CU* scheme an improvement of 27.27% and for the *CI-CU* scheme a maximum localisation improvement of 32.47%. One can see that the improvement in localisation error diminishes when the number of quadrotors exceeds 4 agents. Additionally, one can observe that in general, the *CI-CU Hybrid TDOA-TWR* scheme comes with the lowest RMSE (state & state-estimate), followed by the *CU* and the *simple* schemes, as long as the inter-agent ranging frequency is kept high enough. As a matter of fact, one can observe in Figure 10 that at a low inter-agent ranging frequency of 2 Hz no real localisation improvement is visible and the higher the frequency, the better the performance of the localisation schemes. For example, the localisation improvement associated with the *CI-CU* scheme with 4 quadrotors and inter-agent

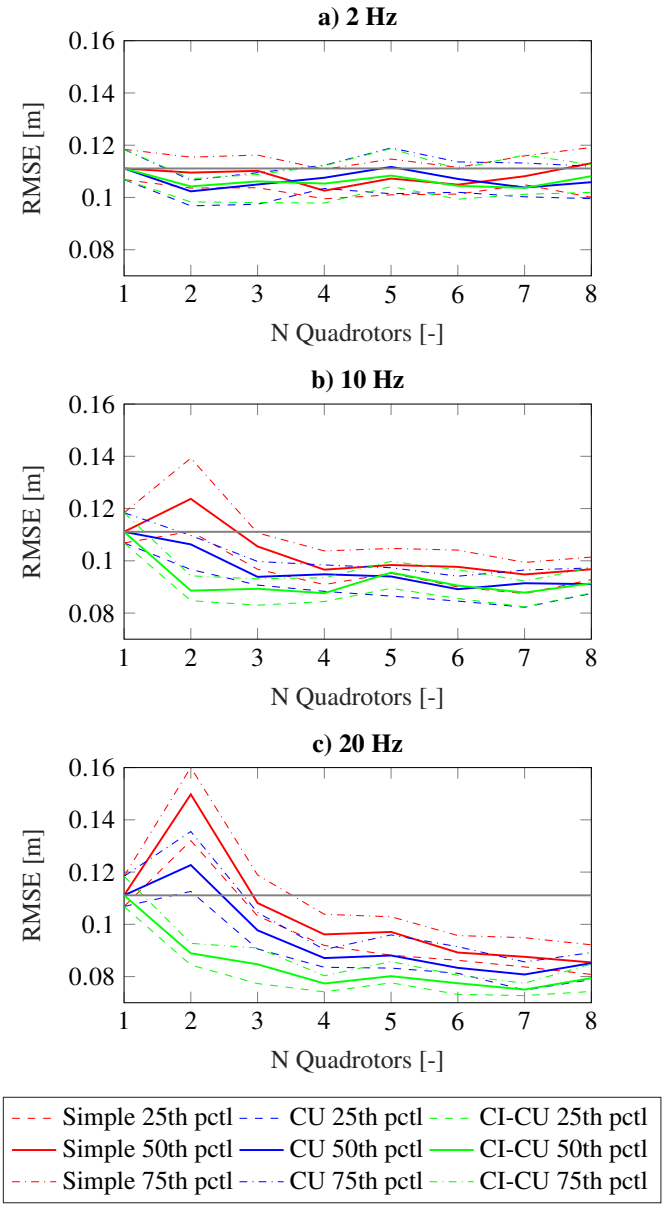

Figure 10. Simulation results for the full-coverage Hybrid TDOA-TWR with varying n of quadrotors and fixed inter-agent ranging frequency of 2 Hz, 10 Hz and 20 Hz (CU = Covariance Updated, CI-CU = Covariance Intersection Covariance Updated).

ranging frequency of 20 Hz is 30.37%, at a frequency of $10Hz$ 21.14% and at a frequency of 2 Hz only 5.21%. Taking a look at the inter-percentile spread of the localisation schemes in Figure 10, one can clearly see that the *CI-CU* scheme comes with the highest stability and performance, followed by the *CU* and *simple* scheme respectively. Additionally, one can also see that the stability of the scheme individually also increases with increasing frequency.

It can also be observed that the improvement between the localisation schemes is rather small. This is to be expected. This is the full-coverage test case, of which the quadrotors are inter-agent ranging at a frequency ranging from $2 - 20$ Hz, while the quadrotors are simultaneously ranging towards static anchors at a much higher frequency of 50 Hz. As the quadrotors are inter-agent ranging at a much lower rate than they are receiving location updates from UWB anchors, their covariance error matrix is not propagating very far in between measurement updates, leaving with a fairly accurate position estimate already. Additionally, due to the fact that the quadrotors are receiving UWB updates from static anchors at a much higher rate than the inter-agent ranging frequency, the rate at which their states are becoming correlated is lower as well. Because of this feat, the cross- and auto-covariance terms remain fairly small and so is the compensation of the error-covariance uncertainty in the measurement noise. These small error-covariance values render small uncertainty compensation values and because of this also a small observed localisation improvement between the schemes.

One can also observe that a higher inter-agent ranging frequency does not always render a lower RMSE between state and state-estimate. As a matter of fact, when two quadrotors are inter-agent ranging, one can observe a deterioration in localisation performance. This can be explained by the fact that the inter-agent ranging frequency in the simulation is kept constant, regardless of the number of quadrotors in the simulation. This means that when two agents are inter-agent ranging their states become correlated at a faster rate than when there are more agents in the simulation at the same inter-agent ranging frequency. Therefore, the first signs of EKF inconsistency —which is a result of the simplifications implemented the localisation schemes— can be seen at a low number of quadrotors and high inter-agent ranging frequency. Additionally, one can see that the *simple* scheme is most prone to this inconsistency, followed by the *CU* and greatly mitigated by the *CI-CU* scheme.

2. Varying inter-agent ranging frequency

Slicing the surface plots obtained for the full-coverage test-case along the n quadrotor axis, one can take a look at the inter-agent ranging performance when varying the inter-agent frequency and keeping the number of quadrotors constant. This helps understanding what happens to the localisation performance when one varies the inter-agent ranging frequency. Slices of the surface plot with varying inter-agent ranging frequencies for respectively 2, 4, 6 and 8 quadrotors are presented in Figure 11. One can observe that in general, a higher TWR frequency comes with a lower observed localisation error, given that the EKF is consistent. This leaves out the cases with low number

of quadrotors and high inter-agent ranging frequency. Additionally, one can see that regardless of the number of quadrotors, the localisation schemes in which uncertainty information is exchanged benefit from a higher TWR frequency and the more uncertainty information is exchanged at that frequency, the higher the benefit. However, with a higher inter-agent ranging frequency, the returns on localisation improvement becomes less. For example, with 6 inter-agent ranging quadrotors, the localisation improvement between the *simple* and *CI-CU* scheme is 3.41% at a frequency of 6 Hz, 5.6% at a frequency of 10 Hz and 6.56% at a frequency of 20 Hz. Once again one can observe that an increase in TWR frequency does not always render a decrease in localisation error. In similar fashion as explained in the previous section, one can observe that when the number of inter-agent ranging quadrotors is low and the inter-agent ranging frequency is high, a deterioration of localisation performance takes place due to inconsistency. In Figure 11 a), one can see that schemes exchanging more uncertainty information render more consistent results and are better at counteracting this deterioration. Please refer to Section III.D for an excursion on the consistency of the EKF and how this can be mitigated.

C. Inter-agent ranging limited-coverage test results

The second round of tests that have been performed are simulated limited-coverage tests. These tests are more relevant than the full-coverage tests, as they represent how the distributed localisation schemes can be used in cases of intermittent UWB anchor reception. There are numerous use-cases where MAV's are flying in an environment where reception of a localisation system is not self-evident and where the deployment of an ad-hoc distributed sensor network consisting of a swarm of MAV's supplemented with some base station anchors can be the solution. Think of the industrial use case of monitoring and inspection of crops in large greenhouses for example. The goal of this series of tests is to present the localisation performance of the localisation schemes when the UWB anchor reception is intermittent. Once again, this series of tests consists of a varying number of quadrotors flying in the simulated test-setup as described in Section III.A. This time, the zone without UWB coverage has been enabled. Outside of the zone the quadrotor has full reception towards the static UWB anchors, inside the zone there is no connection at all to static UWB anchors and the quadrotor is solely relying on its own position estimate (IMU) and inter-agent ranging measurements between swarm members. The quadrotors flying inside the zone without static UWB anchor reception are allowed to range towards quadrotors outside the zone and vice versa. As the intention of these simulated tests is to objectively quantify the performance of the proposed inter-agent ranging schemes, it has been decided to not limit the measurement range between the inter-agent ranging agents. Once again all the test results presented in this section have been performed for the *simple*, *CU* and *CI-CU* inter-agent ranging schemes. Surface plots with the results of the *simple*, *CU* and *CI-CU* inter-agent ranging scheme, can be found in Figures 23, 24 and 25 of Appendix VI respectively.

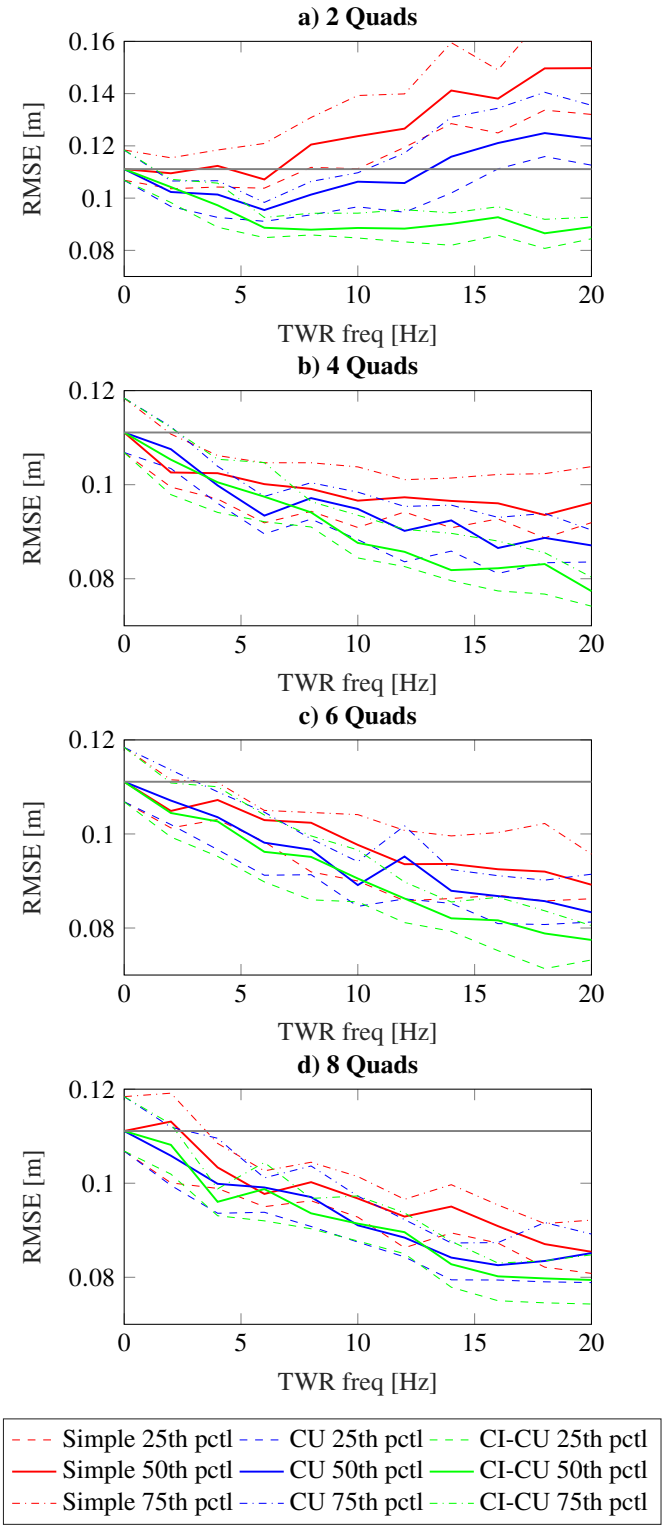

Figure 11. Simulation results for the full-coverage Hybrid TDOA-TWR with varying inter-agent ranging frequency for fixed number of quadrotors of 2, 4, 6 and 8 quadrotors (CU = Covariance Updated, CI-CU = Covariance Intersection Covariance Updated).

1. Varying number of quadrotors

In order to have a better understanding of how a swarm of quadrotors can improve it's location estimate by inter-agent ranging with neighbouring agents in the swarm, one can slice the resulting surface plots along the inter-agent ranging frequency axis. In Figure 13, one can see the limited-coverage simulation results with varying quadrotors, keeping the inter-agent ranging frequency constant at a value of 2, 10 and 20 Hz respectively. Once again, one can observe that the *CI-CU* scheme generally comes with the lowest RMSE (true state & state-estimate) followed by the *CU* and *simple* schemes respectively.

As this time the test-setup involves a zone without UWB reception, the quadrotors have to perform inter-agent ranging in order to compensate for IMU drift inside that zone. One can see that when a single quadrotor is trying to fly the trajectory (without inter-agent ranging measurements), the quadrotors experience extreme drift when crossing the zone without UWB reception. As a matter of fact, the median observed RMSE of a quadrotor flying the trajectory without inter-agent ranging is 0.9 meters. The drifting error of the quadrotor flying through the zone without UWB coverage is dependent on the size of the zone. Such an error has the potential to greatly affect the performance of a real life application. When increasing the number of quadrotors flying the trajectory, one can observe that the localisation error is decreasing.

For example, when simulating the *simple* scheme for 2 quadrotors at an inter-agent ranging frequency of 10 Hz, an improvement of 39.14% can be observed, of 64.22% for 4 quadrotors, 66.36% for 6 quadrotors and 76.31% for 8 quadrotors. Additionally, one can once again observe that the schemes exchanging more uncertainty information come with a lower localisation error. For comparison, when varying the number of quadrotors between $1-8$ for the *CI-CU* scheme, one can observe for an inter-agent ranging frequency of 10 Hz, an average localisation improvement of 40.34% for 2 quadrotors, 75.97% for 4 quadrotors, 79.56% for 6 quadrotors and 81.77% for 8 quadrotors can be observed. One can see that the observed localisation improvement diminishes after adding more than 4 quadrotors. This point is highly dependent on the trajectory and zone without UWB coverage. The quadrotors are distributed over the trajectory presented in Section III.A. When a quadrotor is flying inside the zone without UWB coverage it is able to range towards an agent that does have connection to the static UWB beacons. Basically relaying the UWB network, creating an ad-hoc distributed localisation network.

In absence of inter-agent ranging measurements, the quadrotors inside the zone without UWB reception are drifting and the error between state and state-estimate is increasing with every prediction step. The agents are benefiting from every measurement obtained from agents outside of the zone. Therefore, the problem of inconsistency is here less visible as in the full-coverage test-case. One can say that for the limited-coverage test-case the influence of inconsistency does not have a crucial impact on the localisation performance of this scheme. However, it still exists and this will be discussed in Section III.D.

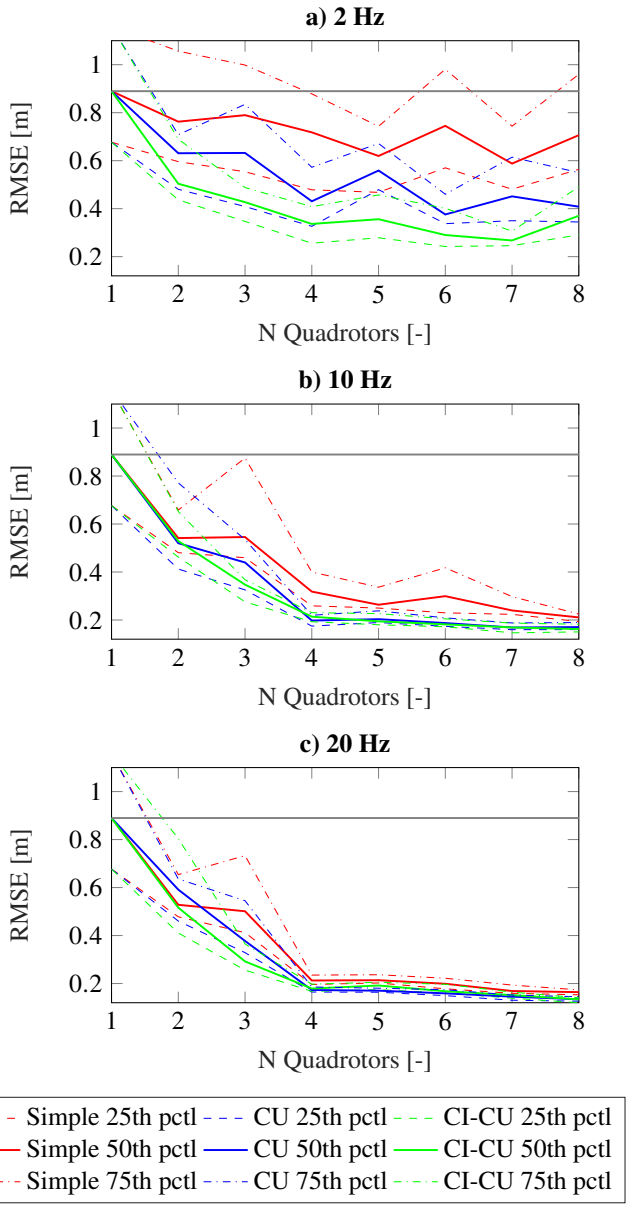

Figure 12. Simulation results for the limited-coverage Hybrid TDOA-TWR with varying n of quadrotors and fixed inter-agent ranging frequency of 2Hz, 10Hz and 20Hz (CU = Covariance Updated, CI-CU = Covariance Intersection Covariance Updated).

2. Varying inter-agent ranging frequency

Once again slicing the surface plots obtained for the limited-coverage test-case along the n quadrotor axis, one can take a look at the inter-agent ranging performance when varying the inter-agent ranging frequency and keeping the number of quadrotors constant. This way one can visualise the impact of increasing the inter-agent ranging frequency when a swarm of quadrotors is flying in an area with limited UWB coverage.

From Figure 13, one can see that in general, with increasing frequency comes a decrease in localisation error. Additionally, one can observe that the rate of improvement in terms of localisation error is decreasing with the increase in inter-agent ranging frequency. For example, for the *simple* scheme with 4 quadrotors, one can observe between 0 and 4 Hz a localisation improvement of 19.29%, between 8 and 12 Hz an improvement of 17.75% and between 16 and 20 Hz, this improvement is only 12.2%. Similarly for *CI-CU* scheme, one can observe between 0 and 4 Hz an average localisation improvement of 62.18%, between 8 and 12 Hz an improvement of 3.81% and between 16 and 20 Hz, this improvement is neglectable. The return on localisation accuracy is diminishing with higher frequency, in a practical application this is an important trade-off factor.

Additionally, the increase in localisation accuracy between the *simple*, *CU* and *CU-CI* schemes is decreasing as well with increasing frequency. For example, the decrease in localisation error for the *CU* scheme in comparison to the *simple* scheme for 8 quadrotors is 47.56% for an inter-agent ranging frequency of 2 Hz, 23.07% for an inter agent ranging frequency of 10 Hz and only 18.38% for an inter-agent ranging frequency of 20 Hz.

D. Inconsistency Excursion

Apart from evaluating the performance of the localisation scheme in terms of absolute positioning error, it is also possible to evaluate the performance of our localisation filter by means of evaluating the average normalized (state) estimation error squared (NEES) during our simulations. The calculation of the NEES values during our simulation is a means of checking the credibility of the error-covariance produced by our filter. By means of the NEES test one tries to figure out whether the estimated error actually approximates the true error. Testing for this criterion is important, as the distributed localisation schemes presented in this paper are greatly simplified in comparison to the centralised usecase. Due to the varying degree of simplifications implemented in the localisation schemes, it can be expected that their susceptibility to inconsistency varies as well. Please refer to Equation 30 for a definition of NEES, according to Huang et al. [16].

$$\epsilon_k = \tilde{x}_k^T P_{k|k}^{-1} \tilde{x}_k \tag{30}$$

with $P_{k|k}$ being the associated sub-matrices of the error covariance matrix P_k corresponding to the quadrotor's position and $\tilde{x}_k$ being represented by the EKF's estimation error here being associated with the quadrotor's ground truth position x_k and estimated position $\hat{x}_k$. Please refer to Equation 31 for a decomposition of this estimation error.

$$\tilde{x}_k = x_k - \hat{x}_k \tag{31}$$

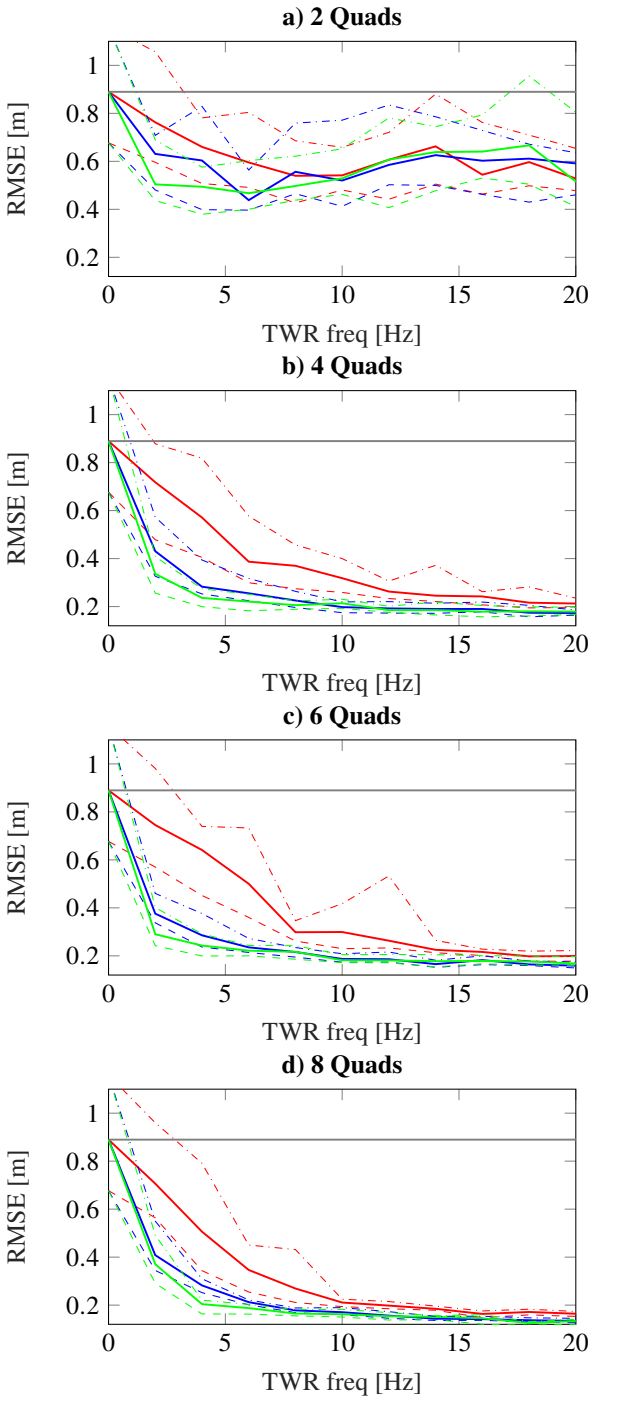

Figure 13. Simulation results for the limited-coverage Hybrid TDOA-TWR with varying inter-agent ranging frequency for fixed number of quadrotors of 2, 4, 6 and 8 quadrotors (CU = Covariance Updated, CI-CU = Covariance Intersection Covariance Updated).

In similar fashion as with the RMSE, the average NEES values have been calculated for both the limited and full coverage test-cases. As explained by Huang et al., it is known that the NEES of a random variable spanning M-dimensions follows a χ^2 distribution [16]. The mean of a χ^2 distribution of dimension M is M. In this case the NEES is evaluated for the x and y position of the quadrotors. The x and y position of the quadrotor is a 2D metric and therefore one can expect optimal values of NEES to be around 2. The higher the NEES value, the larger the inconsistency presented by the filter.

The average NEES values for both the limited- and full-coverage test-case have been calculated and they are presented in Figure 14. The NEES values are plotted with a varying inter-agent ranging frequency between 2 and 20 Hz, for 2, 4, 6 and 8 inter-agent ranging quadrotors respectively. From Figure 14, one can see that with a larger inter-agent ranging frequency, the larger the presented inconsistency of the EKF. Additionally, the presented inconsistency is larger the more simplifications the schemes incorporate. This is to be expected, schemes undergo some major simplifications in comparison to the ideal distributed EKF. This has been presented in Section II.C. Therefore, with every measurement update, inconsistency of the EKF is provoked. The higher the inter-agent ranging frequency, the more measurement updates, the more inconsistent the EKF becomes.

It can be observed that the consistency can be delayed and decreased. As the inter-agent ranging frequency is kept constant for every agent in the swarm, the rate at which the states of the swarm agents become correlated decreases not only with the inter-agent ranging frequency, but also with the number of quadrotors in range. Therefore, having a dense swarm of MAV's can help delaying the inconsistency problem. It can also be observed that the full-coverage test-case does not suffer from the same level of consistency problems as the limited-coverage test-case. This can be explained by the fact that the limited-coverage test-case undergoes major drift when the quadrotors are flying in the zone without UWB anchor coverage. In Figure 14, one can clearly see that at a high number of quadrotors, inconsistency is drastically decreased with the uncertainty exchanging schemes as opposed to the simple approach. This shows that compensating for uncertainty measures has favourable results.

The degree of inconsistency improvement of the localisation schemes is dependent on many factors. The better uncertainty compensation in the ranging measurement, the smaller the inter-agent ranging inconsistency problem becomes. Additionally, one also has to take into account the model being used in the propagation step of the quadrotor's EKF. The localisation schemes assume that the filter on the ranging quadrotor is consistent, meaning that one assumes zero-mean estimation errors and a covariance matrix of the output that is slightly smaller or equal to the calculated covariance matrix. The better the output of the model approximates the quadrotor's behaviour, the better the representation of the error-covariance matrix becomes in times of drift (multiple sequential prediction steps), the lower inconsistency presented when the quadrotor has no UWB coverage.

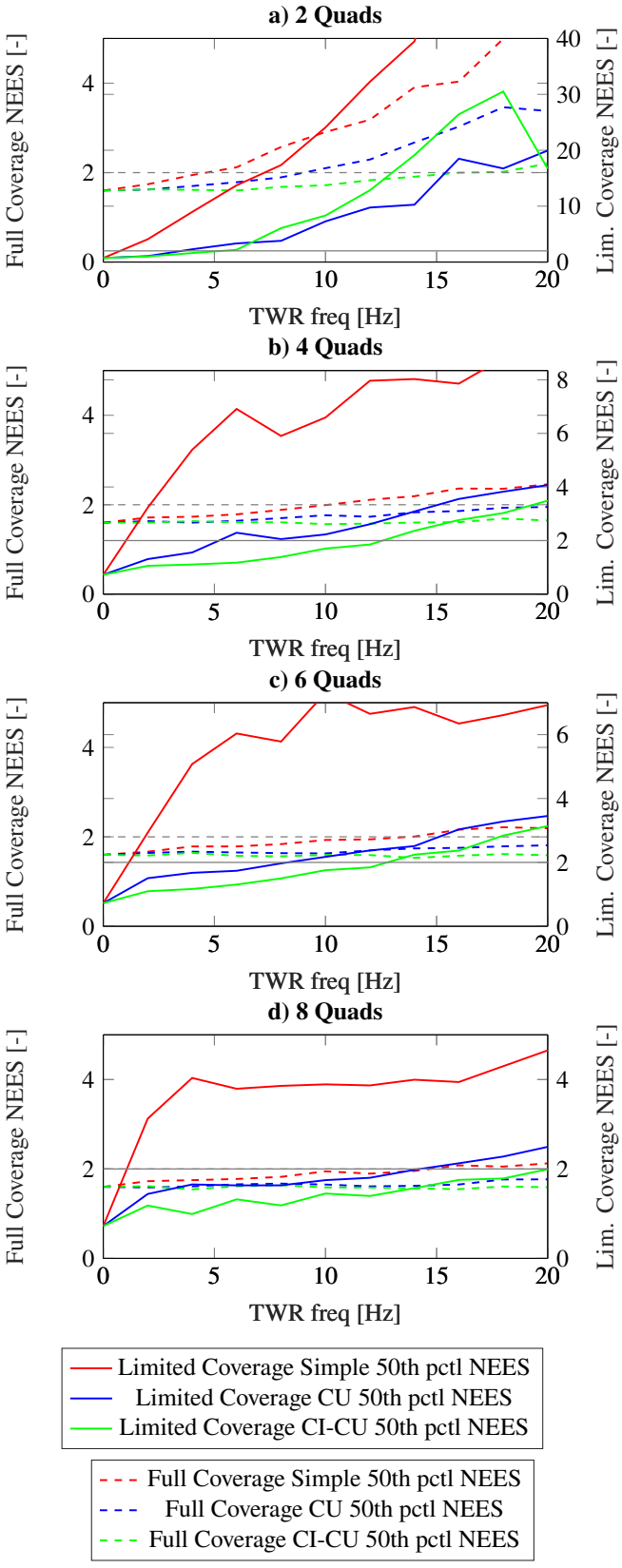

Figure 14. Simulation results for the full- and limited-coverage Hybrid TDOA-TWR NEES values with varying inter-agent ranging frequencies for fixed number of quadrotors of 2, 4, 6 and 8 quadrotors (CU = Covariance Updated, CI-CU = Covariance Intersection Covariance Updated). NEES of value 2 indicated in gray.

IV. Cyberzoo Test Results & Discussion

In this Chapter, the performance of the *simple*, *CU* and *CU-CI Hybrid TDOA-TWR* localisation schemes will be evaluated in practice. The purpose of this chapter is to validate the simulations and methods presented in Section II and III. First, in Section IV.A, the test-setup will be presented. This entails a description of the testing environment, as well as the hardware used for this research. Next, in Section IV.B, the results of the practice tests will be presented and discussed.

A. Cyberzoo test-setup

The validation tests have been performed at the TU Delft Cyberzoo. This is a micro air vehicle test facility at the TU Delft faculty of Aerospace Engineering, where one can test a wide variety of unmanned air vehicles (UAV) in a safe manner. It has been decided to use the Crazyflie 2.1 as platform for the practice tests. The Crazyflie 2.1 is a lightweight quadrotor that can be equipped with various sensors and can run custom scripts in order to change it's behaviour. The Cyberzoo is equipped with an Optitrack system that will be used for ground truth recording.

The ecosystem of Bitcraze makes it possible to equip the Crazyflie with all the necessary sensors for this research. For the tests performed in this research a total of 4 Crazyflies have been used. Each of the Crazyflies are equipped with two Loco-positioning UWB decks and one Flowdeck v2. The first Loco-positioning deck is used to perform TDOA with the static UWB anchors of the Cyberzoo, while the second Loco-positioning deck is used to perform TWR with the swarm members. Additionally, the Flowdeck v2 provides optical flow measurements and is used for height control and limiting drift in absence of UWB measurements. Hosting this many sensors is a highly unsupported configuration, requiring adapted wiring and adjustments to the firmware. For full integration with the Bitcraze ecosystem, the Crazyflie client has been adapted to accommodate these changes as well.

Due to the fact that the Crazyflie is carrying an unsupported payload the Crazyflie is flying close to it's maximum take-off weight. The advertised maximum take-off weight of a Crazyflie 2.1 is 42g, of which the Crazyflie itself is 27g. This leaves 15g of useful payload. The 2 UWB decks (3.3g each), Flowdeck v2 (1.6g) and battery (7.1g) account for a total payload of 15.3g. This means that the Crazyflie is loaded to its limits and this greatly affects the stability of the system during take-off and flight manoeuvres. For example, if the voltage drop of the battery is higher than 0.8v or the motors are not perfectly balanced anymore, the Crazyflie crashes when giving full thrust. The flight time of the Crazyflie is also highly reduced to a maximum of 3 minutes. Additionally, when flying 4 Crazyflies in the Cyberzoo, high levels interference on the radio channel take place (regardless of distributing channels), making the swarm hard to control. An extension to the ceramic antenna of the Crazyflie has been implemented and this partially solved the issue. Nevertheless, due to the limited stability of the test-setup, only a specific test-case with 4 quadrotors has been tested.

B. Test results

The main test will be a limited coverage test, in which the application of the three inter-agent ranging schemes (simple, CU, CI-CU) has been tested in practice. In similar fashion as with the simulated tests, the 4 Crazyflies will fly an approximated square of 4×4 meters in clockwise direction. The 4 quadrotors will fly the square trajectory simultaneously, while being evenly distributed on the trajectory. While flying the trajectory, the 4 Crazyflies will perform TDOA localisation with static anchors in the Cyberzoo and inter-agent ranging in between the swarm members. Since the Cyberzoo is too small to leave the range of the static UWB anchors, a zone in which the Crazyflie does not have connection to the static UWB anchors is implemented, emulating a limited-coverage environment. Inside that zone, the Crazyflie does not have connection to the static UWB anchors anymore and has to rely on inter-agent ranging measurements between the swarm members to compensate for drift. Please refer to Figure 15 for a representation of this test trajectory. This test-case makes it possible to evaluate the performance of the localisation scheme when the UWB connection is intermittent. Imagine that the test-setup is a greenhouse with UWB reception on the sides, but no UWB connection in the middle of the field.

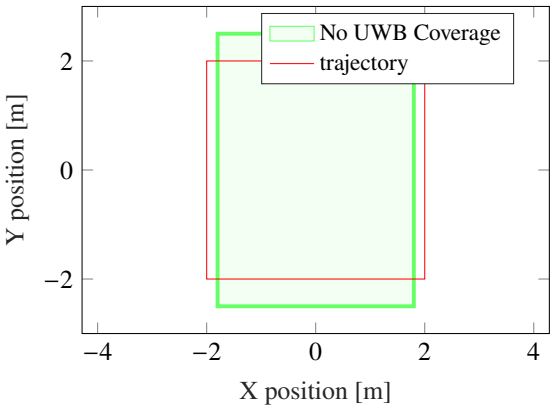

Figure 15. Visualisation of the limited-coverage Cyberzoo test-setup.

Above trajectory has been flown at least 2 times consecutively for every localisation scheme and at least 5 batches for every scheme were recorded. Additionally, the trajectory has been flown as well with 1 quadrotor without inter-agent ranging capabilities. This way one can clearly illustrate the advantage of our inter-agent ranging approaches above drifing across the area without coverage. Please refer to Figures 26 to 29 of Appendix VI for a qualitative visualisation of the tests. Although the improvement in localisation performance between the schemes is subtle, it is still visually noticeable. Additionally, the average of the test runs for every test-scenario can be found in the bar plot in Figure 16.

From Figure 16, one can clearly see that by exchanging more information, the localisation performance of the swarm improves. As a matter of fact, the average RMSE without inter-agent ranging was found to be 0.44 meters, while the average RMSE of the simple, CU, and CI-CU schemes were found to be 0.28, 0.17 and 0.13 respectively. Additionally, an increase in

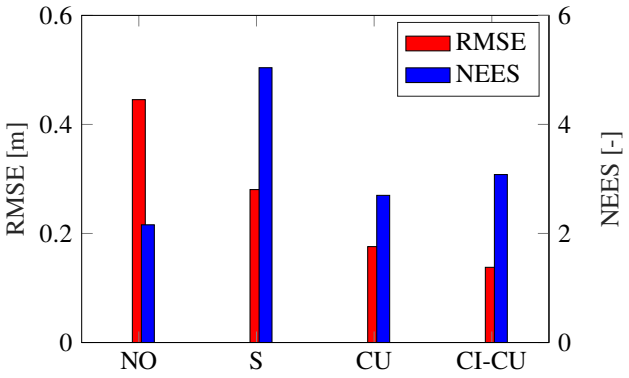

Figure 16. Cyberzoo test results for the Simple (S), Covariance Updated (CU) and Covariance Intersection Covariance Updated (CI-CU) localisation schemes with 4 MAV's compared to no ranging (NO)

average normalised state-estimation error squared (NEES) could be seen when comparing the no inter-agent ranging case and the simple case, with an expected decrease for the CU and CI-CU localisation schemes. It can also be seen that no significant decrease in NEES can be observed between the CU and CI-CU test-case. This can be explained by the fact that the Crazyflies are inter-agent ranging at a rather low frequency of around $\approx$ 10 Hz. Additionally, the Crazyflies are receiving optical flow measurements from the Flowdeck v2, keeping the estimated covariance in bounds. The NEES is also calculated based on the covariance values and the error between state-estimate and ground truth. The ground truth is obtained through Optitrack measurements and these have shown to have some variation in them as well. It can be seen that as long as the inter-agent ranging frequency is kept low, the CI-CU scheme gives little advantage to the CU scheme in terms of reducing inconsistency.

In order to showcase the other possibilities of the presented inter-agent ranging schemes, it has been decided to emulate above test-scenario in a small-scale greenhouse test. This time a greenhouse with limited UWB coverage is simulated in the Cyberzoo. Once again, this test is performed with 4 Crazyflies. This time, 3 Crazyflies hover stationary in the zone with static UWB anchor connection. These can be seen as Crazyflies flying at the borders of the greenhouse field, still in connection with UWB beacons placed around the crops. The fourth Crazyflie is performing a task in the middle of the greenhouse (e.g. scanning a crop). In the middle of the greenhouse there is no connection to the static UWB anchors. Instead, Crazyflie number 4 has to rely on inter-agent ranging measurements with agent 1-3 to receive an absolute location update. In the meantime, all of the Crazyflies are inter-agent ranging with each other. Crazyflies 1-3 are basically relaying the UWB network, extending the reach of the UWB network, allowing Crazyflie 4 to receive an absolute localisation update in a zone without static UWB anchor connection. Please refer to Figure 17 for a depiction of this test-setup.

In Figure 18, one can see the amount of drift a single Crazyflie experiences when it does not have connection to static UWB anchors and is not performing inter-agent ranging measurements with its peers. One can see that the quadrotor experiences large

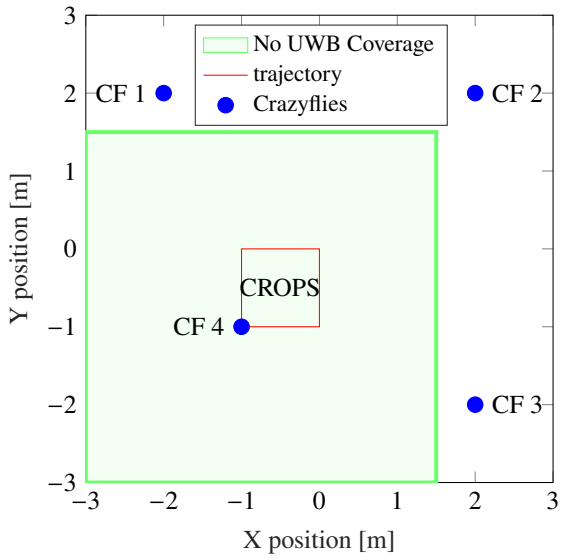

Figure 17. Visualisation of the small scale greenhouse test-setup.

amounts of drift and the location estimate deteriorates quickly. This flown trajectory has an associated RMSE of about 0.6 meters between ground truth and state-estimate.

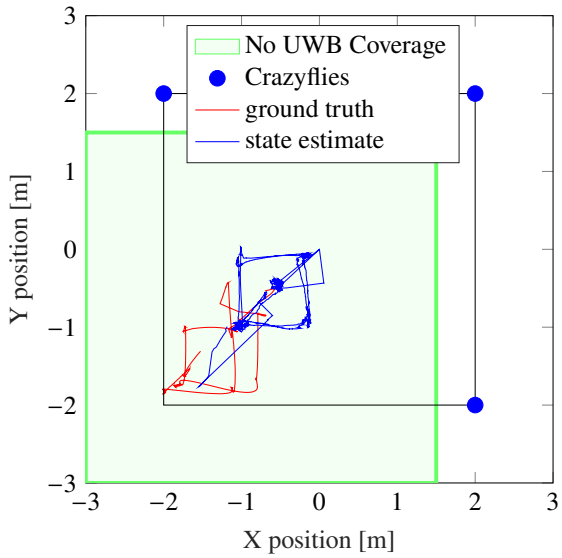

Figure 18. Visualisation of the small scale greenhouse test with 4 Crazyflies and no inter-agent ranging

In Figure 19, one can see the performance of the CU localisation scheme when a Crazyflie is flying in a zone without UWB connection and relies on inter-agent ranging measurements received from its peers. One can see an improvement in performance with an associated RMSE of about 0.29 meters. During testing it has been found that the performance of the simple, CU and CI-CU localisation schemes were comparable. Therefore only the result for the CU localisation scheme is shown. The explanation for these comparable results are due to the fact that CF 1-3 are in constant connection to the static UWB anchors. This results in an accurate position fix for these Crazyflies,

keeping their covariance estimates low. Due to this low uncertainty, augmenting the measurement noise with the covariance of the ranging agent results in marginal improvements. Ideally, the location estimate of Crazyflies 1-3 would experience some deterioration when not compensating for the uncertainty of quadrotor 4 in the inter-agent ranging measurements. However, as UWB measurement update rate with the static UWB anchors for CF 1-3 is of a greater magnitude than the inter-agent ranging measurements, this deterioration is very small and difficult to record with the available hardware.

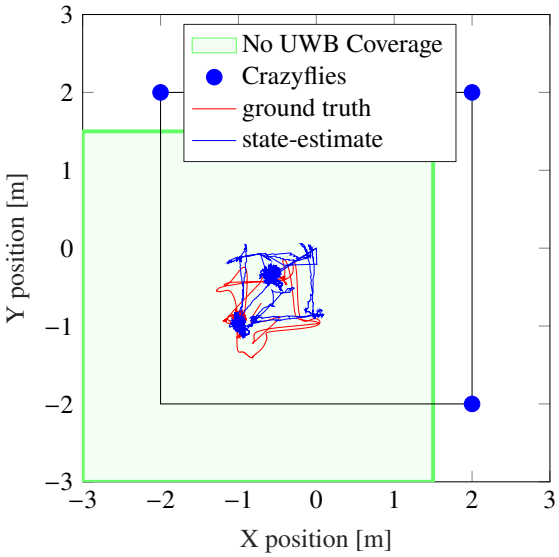

Figure 19. Visualisation of the small scale greenhouse test with 4 Crazyflies and Covariance Updated (CU) inter-agent ranging

In the ideal scenario, above tests are reproduced in a larger area and the ground truth is logged for every agent of the swarm. This way one can clearly record the fact that exchanging uncertainty information between the swarm members prevents localisation deterioration for agents with static UWB anchor connection and improves localisation performance for agents in a zone without static UWB anchor connection.

V. Conclusion & Recommendations

In this work the performance of a distributed and scalable localisation system with minimal reliance on static localisation hardware has been evaluated both in simulation and in practice. For the generation of the simulated results, a modular Simulator designed for the testing of UWB swarming localisation schemes has been developed on the backbone of Swarmulator. In order to perform the practice tests in the Cyberzoo, a custom Crazyflie 2.1 has been developed as well. It has been found that when augmenting the measurement noise of UWB ranging measurements with the uncertainty associated with the ranging quadrotor, an improvement in localisation performance can be observed. In simulation this has been found to be true for an environment with full UWB coverage and limited UWB coverage. In practice, these improvements could only be observed for an area with limited UWB coverage. Full UWB coverage improvements could not be recorded in practice due to the fact that these improvements are small and difficult to capture.

A total of three inter-agent ranging schemes were presented: simple, covariance updated (CU) and covariance intersection covariance updated (CI-CU). In simulation it has been found that in general, the CI-CU scheme comes with the best performance, followed by the CU and the simple schemes respectively, both in terms of localisation error (RMSE) and filter consistency (NEES). In practice, it has been found that in terms of localisation error the CI-CU scheme also has the best performance, followed by the CU and simple schemes. However, this time the performance of the CI-CU scheme and the CU scheme were on par in terms of filter consistency. In an attempt to show a practical application of the inter-agent ranging schemes, a small scale greenhouse test has been performed. This test has shown that inter-agent ranging by a swarm of micro air vehicles can render powerful results given the right practical implementation.

By performing both tests in simulation and in practice, an attempt has been made at crossing the reality gap. This has proven to be difficult and with these proper recommendations for future work can be made. The simulator used for the simulations in this paper is properly tuned such that the simulated quadrotors are stable and its filters are consistent. It has been found that the Crazyflie 2.1 does not feature this stability or consistency. In future work, both the hardware and the firmware should be revisited. On the hardware side the reliability of the system should be increased. This involves increasing the useful payload and flight time of the system. An example solution for this would be a redesign of the airframe and the implementation of brushless motors. Additionally, one could increase the reliability of the custom sensor setup by multiplexing the useful pins of the Crazyflie 2.1. With this more capable Crazyflie, one can also implement on-board logging, reducing the experienced interference issues. On the software side the inter-agent ranging scheduling technique can be revisited. This way the inter-agent ranging frequency can be increased and the performance of the inter-agent ranging schemes can be re-evaluated for these higher frequencies. Additionally, this scheduling technique can allow for a swarm with changing number of members, making the localisation scheme fully scalable. The Crazyflie's sensor fusion system and Flowdeck v2 implementation should also be revisited such that the Crazyflie renders a more representable covariance estimate. Once the hardware and software improvements have been implemented, it is possible to couple this localisation system with an associated swarming behaviour, showcasing the full power of this distributed localisation scheme. One could for example use this localisation scheme for the inspection of crops in large greenhouses. This way an ad-hoc localisation system could be deployed without extensive installation of infrastructure.

Acknowledgments

I would like to thank my supervisor S.U. Pfeiffer and Dr. G.C.H.E. de Croon for their guidance and valuable feedback during this thesis project. I also greatly enjoyed my time at the TU Delft MAV lab and the numerous interesting conversations with its researchers. I also would like to thank my girlfriend and parents for their ongoing support over the last year.

References

[1] Brambilla, M., Ferrante, E., Birattari, M., and Dorigo, M., "Swarm robotics: a review from the swarm engineering perspective," *Swarm Intelligence*, Vol. 7, No. 1, 2013, pp. 1–41. doi: 10.1007/s11721-012-0075-2, URL http://link.springer.com/10.1007/s11721-012-0075-2.

[2] Bitcraze, "Loco Positioning System," https://www.bitcraze.io/documentation/system/positioning/loco-positioning-system/, April 2022.

[3] Alarifi, A., Al-Salman, A., Alsaleh, M., Alnafessah, A., Al-Hadhrami, S., Al-Ammar, M. A., and Al-Khalifa, H. S., "Ultra wideband indoor positioning technologies: Analysis and recent advances," *Sensors (Switzerland)*, Vol. 16, No. 5, 2016, pp. 1–36. doi: 10.3390/s16050707.

[4] Papastratis, I., Charalambous, T., and Pappas, N., "Indoor Navigation of Quadrotors via Ultra-Wideband Wireless Technology," *Proceedings - 2018 Advances in Wireless and Optical Communications, RTUWO 2018*, 2018, pp. 106–111. doi: 10.1109/RTUWO.2018.8587889.

[5] Al-Ammar, M. A., Alhadhrami, S., Al-Salman, A., Alarifi, A., Al-Khalifa, H. S., Alnafessah, A., and Alsaleh, M., "Comparative survey of indoor positioning technologies, techniques, and algorithms," *Proceedings - 2014 International Conference on Cyberworlds, CW 2014*, , No. September 2018, 2014, pp. 245–252. doi: 10.1109/CW.2014.41.

[6] Liu, H., Darabi, H., Banerjee, P., and Liu, J., "Survey of wireless indoor positioning techniques and systems," *IEEE Transactions on Systems, Man and Cybernetics Part C: Applications and Reviews*, Vol. 37, No. 6, 2007, pp. 1067–1080. doi: 10.1109/TSMCC.2007.905750.

[7] Gezici, S., and Poor, H. V., "Position estimation via ultra-wideband signals," *Proceedings of the IEEE*, Vol. 97, No. 2, 2009, pp. 386–403. doi: 10.1109/JPROC.2008.2008840.

[8] Farid, Z., Nordin, R., and Ismail, M., "Recent advances in wireless indoor localization techniques and system," *Journal of Computer Networks and Communications*, Vol. 2013, 2013. doi: 10.1155/2013/185138.

[9] Ledergerber, A., Hamer, M., and D'Andrea, R., "A robot self-localization system using one-way ultra-wideband communication," *IEEE International Conference on Intelligent Robots and Systems*, Vol. 2015-Decem, 2015, pp. 3131–3137. doi: 10.1109/IROS.2015.7353810.

[10] Coppola, M., "Lightweight C++ simulator for simulating swarms," https://github.com/coppolam/swarmulator, April 2022.

[11] Matlab, "Matlab waypoint trajectory system object," https://www.mathworks.com/help/fusion/ref/waypointtrajectory-system-object.html, May 2022.

[12] IEEE Robotics and Automation Society., *2005 IEEE International Conference on Robotics and Automation (ICRA) : Barcelona, Spain : 18-22 April, 2005.*, IEEE, 2005.

[13] Bitcraze, "Crazyflie 2.0 System," https://www.bitcraze.io/products/old-products/crazyflie-2-0/, April 2022.

[14] Roumeliotis', S. I., and Bekey', G. A., "Collective Localization: A distributed Kalman filter approach to localization of groups of mobile robots*," , 2000.

[15] Roumeliotis, S. I., and Bekey, G. A., "Distributed multirobot localization," *IEEE Transactions on Robotics and Automation*, Vol. 18, No. 5, 2002, pp. 781–795. doi: 10.1109/TRA.2002.803461.

[16] Huang, G. P., Mourikis, A. I., and Roumeliotis, S. I., "Analysis and improvement of the consistency of extended Kalman filter based SLAM," *Proceedings - IEEE International Conference on Robotics and Automation*, , No. 612, 2008, pp. 473–479. doi: 10.1109/ROBOT.2008.4543252.

[17] Julier, S. J., and Uhlmann, J. K., "New extension of the Kalman filter to nonlinear systems," *Signal Processing, Sensor Fusion, and Target Recognition VI*, Vol. 3068, No. July 1997, 1997, p. 182. doi: 10.1117/12.280797.

[18] Goel, S., Kealy, A., Gikas, V., Retscher, G., Toth, C., Brzezinska, D.-G., and Lohani, B., "Cooperative Localization of Unmanned Aerial Vehicles Using GNSS, MEMS Inertial, and UWB Sensors," *Journal of Surveying Engineering*, Vol. 143, No. 4, 2017, p. 04017007. doi: 10.1061/(asce)su.1943-5428.0000230.

[19] Arambel, P. O., Rago, C., and Mehra, R. K., "Covariance intersection algorithm for distributed spacecraft state estimation," *Proceedings of the American Control Conference*, Vol. 6, 2001, pp. 4398–4403. doi: 10.1109/acc.2001.945670.

[20] Klingner, J., Ahmed, N., and Correll, N., "Fault-tolerant Covariance Intersection for localizing robot swarms," *Robotics and Autonomous Systems*, Vol. 122, 2019, p. 103306. doi: 10.1016/j.robot.2019.103306, URL https://doi.org/10.1016/j.robot.2019.103306.

[21] Fränken, D., and Hüpper, A., "Improved fast covariance intersection for distributed data fusion," *2005 7th International Conference on Information Fusion, FUSION*, Vol. 1, 2005, pp. 290–297. doi: 10.1109/ICIF.2005.1591849.

[22] Pfeiffer, S., "Data underlying the publication: A computationally Efficient Moving Horizon Estimator for UWB Localisation on Small Quadrotors," https://data.4tu.nl/articles/dataset/Data_underlying_the_publication_A_Computationally_Efficient_Moving_Horizon_Estimator_for_UWB_Localization_on_Small_Quadrotors_/14827680, June 2022.

VI. Appendix

Table 1. Parameters of simulated Crazyflie

Crazyflie Parameter	Value
mass	0.022 $[kg]$
arm length l	0.042 $[m]$
Jx (around rot. axis)	0.0000091914 $[kg \cdot m^2]$
Jy (around rot. axis)	0.0000091914 $[kg \cdot m^2]$
Jz (around rot. axis)	0.0000228 $[kg \cdot m^2]$

Table 2. Coordinates of static UWB anchors for the simulated test-setup

Anchor ID	x-pos [m]	y-pos [m]
0	-12	-1.5
1	12	-1.5
2	-12	-3
3	12	-3
4	-12	1.5
5	12	1.5
6	-12	3
7	12	3

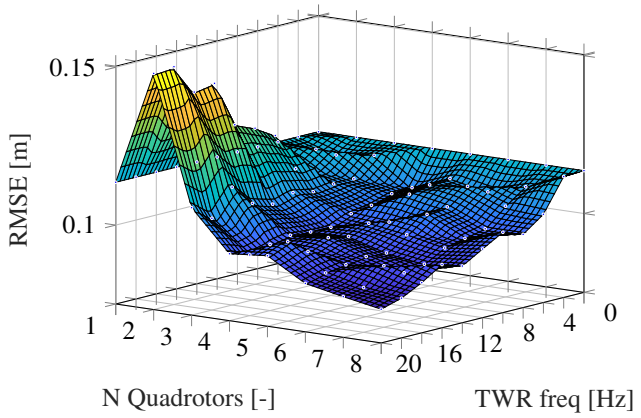

Figure 20. Full-coverage Simple Hybrid TDOA-TWR with varying n of quadrotors and varying inter-agent ranging frequency

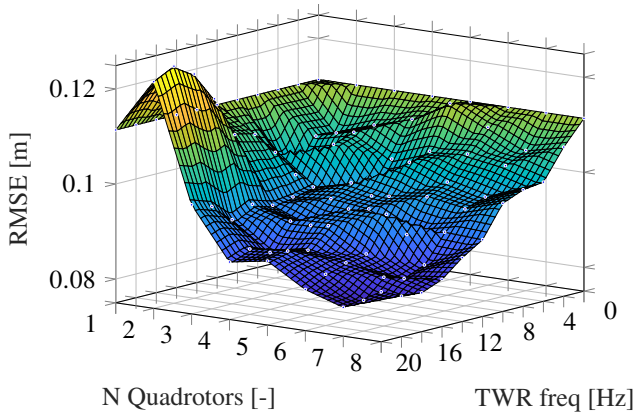

Figure 21. Full-coverage CU Hybrid TDOA-TWR with varying n of quadrotors and varying inter-agent ranging frequency (CU = Covariance Updated)

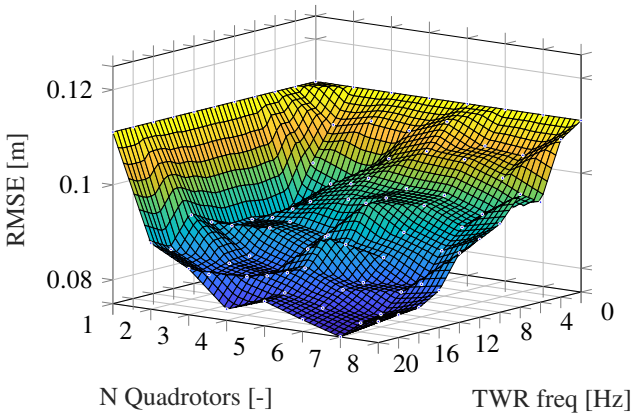

Figure 22. Full-coverage CI-CU Hybrid TDOA-TWR with varying n of quadrotors and varying inter-agent ranging frequency (CI-CU = Covariance Intersection Covariance Updated)

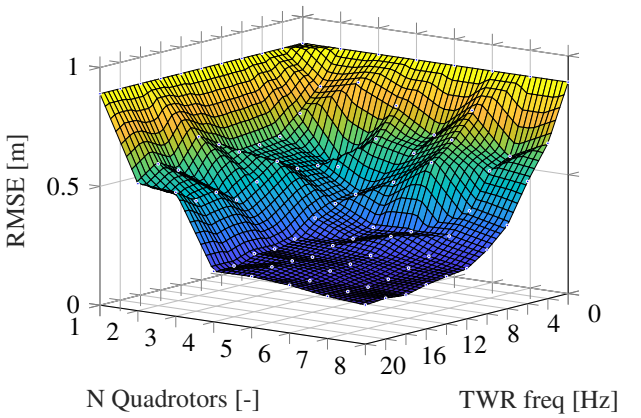

Figure 23. Limited-coverage Simple Hybrid TDOA-TWR with varying n of quadrotors and varying inter-agent ranging frequency

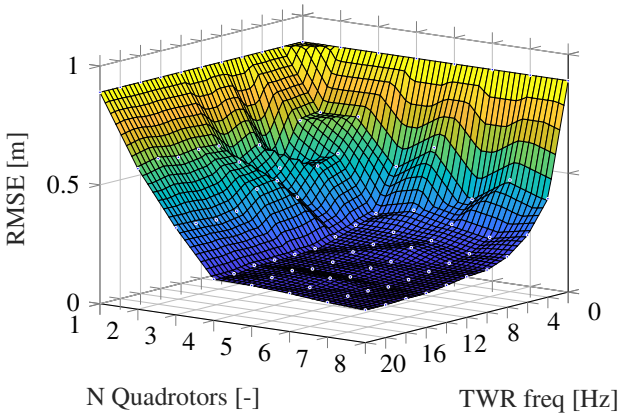

Figure 24. Limited-coverage CU Hybrid TDOA-TWR with varying n of quadrotors and varying inter-agent ranging frequency (CU = Covariance Updated)

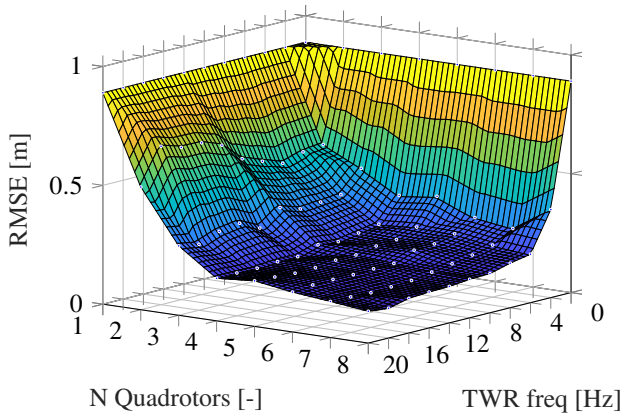

Figure 25. Limited-coverage CI-CU Hybrid TDOA-TWR with varying n of quadrotors and varying inter-agent ranging frequency (CI-CU = Covariance Intersection Covariance Updated)

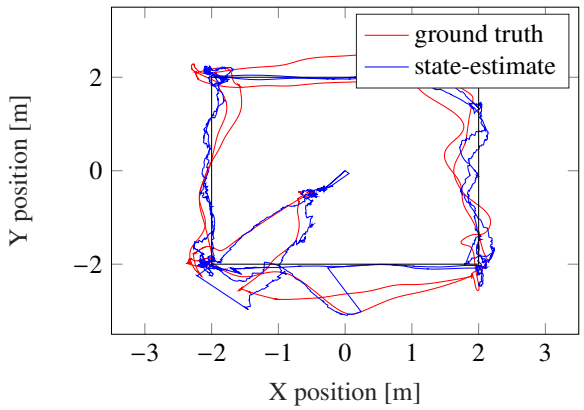

Figure 26. Limited-coverage 1 MAV no inter-agent ranging Cyberzoo test

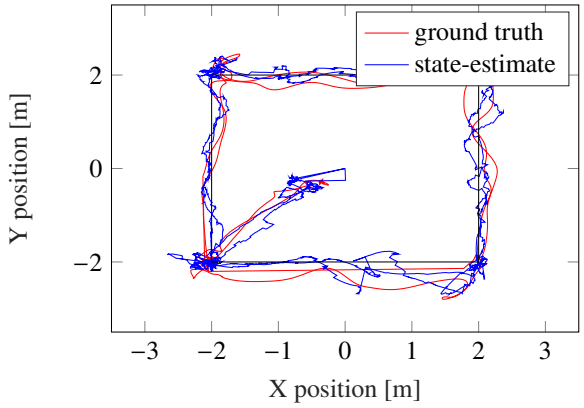

Figure 27. Limited-coverage 4 MAV's Simple Hybrid TDOA-TWR Cyberzoo test

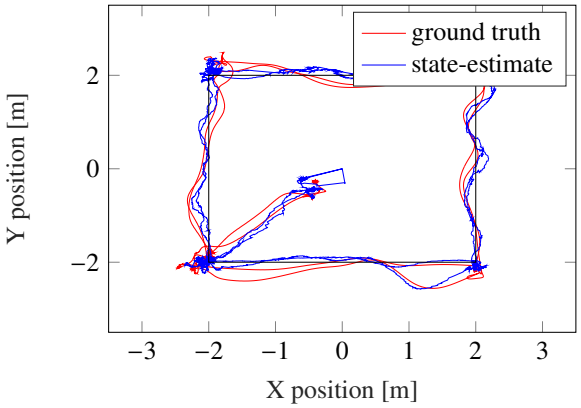

Figure 28. Limited-coverage 4 MAV's CU Hybrid TDOA-TWR Cyberzoo test (CU = Covariance Updated)

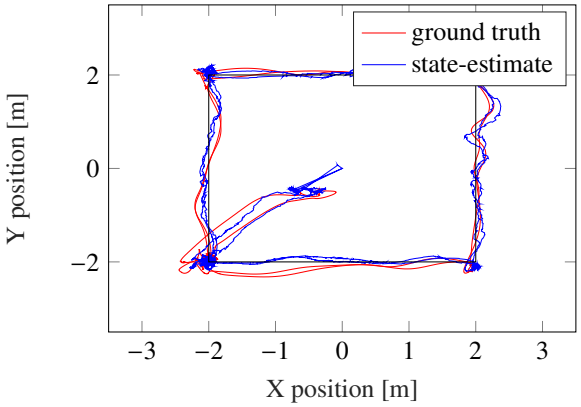

Figure 29. Limited-coverage 4 MAV's CI-CU Hybrid TDOA-TWR Cyberzoo test (CI-CU = Covariance Intersection Covariance Updated)

2

Additional Developments

In this extra appendix additional developments that were part of this master thesis work will be discussed. The tools that are part of these developments are highly relevant for this research but can be very useful for further research as well. First, in Section 2.1 the additional developments on the Swarmulator platform will be presented, as well as the possibilities for future work, after which, in Section 2.2, the customised Crazyflie 2.1 and it's tools will be presented as well. This allows the reader to recreate the test-setup for his own research or for replication purposes. Please find all of the developments on the thesis Github repository[1].

2.1. Swarmulator

The Swarmulator simulator is a lightweight micro air vehicle behaviour simulator developed in C++[2]. It is a modular simulator that allows the user to test schemes for swarming behaviour in a structured way. It is possible to develop your own simulated agent and accompanying behavioural controller. However, out of the box the original Swarmulator does not accommodate elaborate quadrotor dynamics, accompanying sensors and sensor fusion or state-estimation filters. Therefore, it has been decided to fork Swarmulator and develop an extended version accommodating these functionalities, without breaking the original functionality of the behavioural simulator. Please find the diagram of these additional functionalities itemised below and illustrated in Figure 2.1.

- **UWB setup**

The basic functionality of the UWB based Loco Positioning System designed by Bitcraze has been implemented. Currently the simulated UWB localisation system supports a TWR, TDOA and the hybrid TWR-TDOA localisation schemes used for this research. Every beacon runs in its own thread, allowing for full independent generation of it's measurements. At compile time, the desired localisation algorithm can be chosen and in a similar modular way as with the modules of the original Swarmulator, it is possible to implement your own localisation scheme. Additionally, the UWB signal characteristics can be set in a preferences file, without recompiling the simulator (anchor locations, inter-agent ranging toggle, signal length, frequency preferences, inter-agent ranging algo, UWB signal noise...).

- **Trajectory generator**

Every quadrotor that is spawned in the Simulator follows a predefined trajectory. The simulator automatically recognises when a trajectory file is loaded with the quadrotor ID in its name (xytrajectory$n$.txt) and the respective trajectory is loaded. Next, the PID trajectory controller steers the state-estimate towards the desired trajectory. The PID values can once again be adjusted without recompilation. For future work it is possible to swap out the trajectory module for a behavioural controller, merging the simulator's new functionalities with the old.

[1] `https://github.com/FrdrcDpn/UWB_loc_thesis.git`
[2] `https://github.com/coppolam/swarmulator`

- **Simplified Quadrotor dynamics and PID controller**

In order to simulate representative quadrotor behaviour in the 2D simulator environment, a quadrotor's physical model has been implemented, only modelling the torques over the quadrotor's degrees of freedom. For simplification purposes, the yaw angle and motion in z-direction are set to zero. The PID controller of the quadrotor is subdivided in a linear and angular control system and steers the state-estimate towards the desired trajectory. The inner PID controller controls the required rotations to achieve the desired torques for the linear displacement, while the outer PID controller steers the acquired linear displacement from the state-estimator towards the desired trajectory. All of the quadrotor's parameters and controller parameters have been set in a preferences file and can be changed without re-compilation.

- **Sensors and EKF state-estimator**

For sensor fusion an EKF state-estimator has been written. Every quadrotor run's its own EKF in its own thread. The quadrotor receives accelerometer measurements for its prediction step and the measurement update step depends on the available UWB measurements. The state-estimator has been written in a modular way, such that one can easily add or remove sensors from the estimator. Additionally, it is also possible to swap out the estimator for the estimator of choice. Once again, all of the state-estimator's parameters can be changed in a preference file, without recompilation of the simulator.

- **New compilation flags**

Apart from the many new preferences that one can set in the simulator's preference file, one also has to compile the simulator with some extra compilation flags. With the flag `CONTROLLER=UWBSIM_controller` one can set the EKF state-estimator and trajectory follower, with `AGENT=quadrotor` one selects the quadrotor dynamics and with `BEACON=beacon_hybrid_extra`, one selects the desired UWB algorithm. This augments the full compilation code to the following:

```
make clean && make CONTROLLER=UWBSIM_controller AGENT=quadrotor
 BEACON=beacon_hybrid_extra ANIMATION=OFF LOG=ON
```

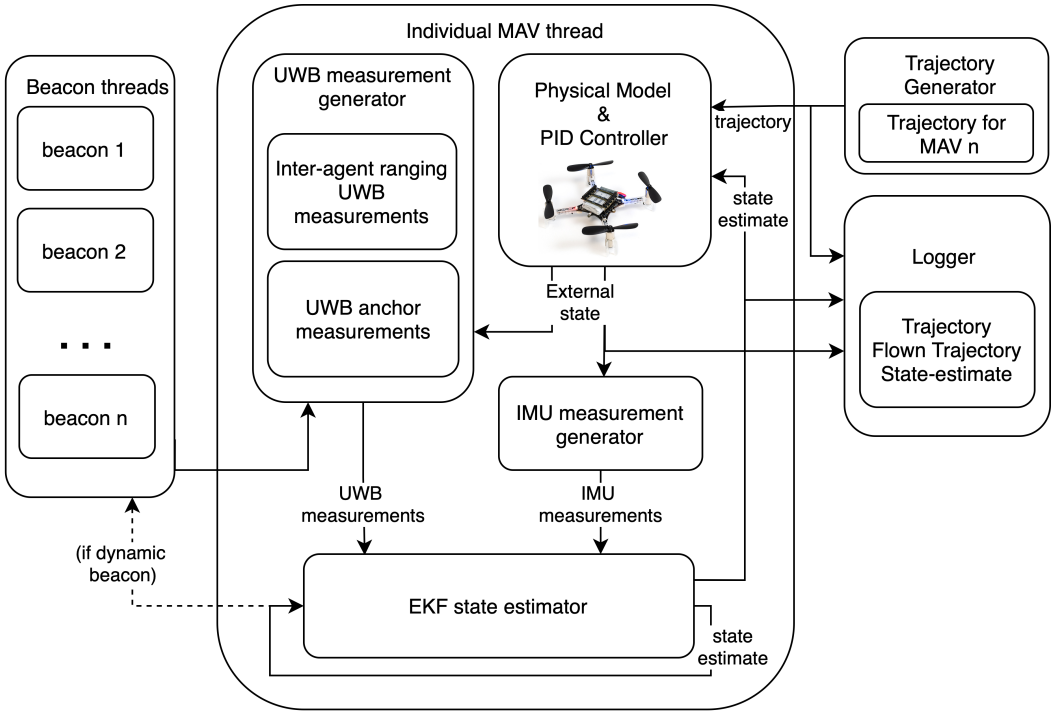

Figure 2.1: Swarmulator extra functionality diagram

2.2. Customised Crazyflie v2.1

A custom Crazyflie v2.1 firmware has been written with support for two Loco Positioning UWB decks and one flodeck v2. In this section an overview will be given of these developments and all the necessary information will be given to replicate this setup. First, the firmware with its additional quircks and features will be presented after which some supporting software developments will be presented as well. Finally, the Crazyflie's custom wiring diagram is shown as well.

- **Crazyflie v2.1 firmware**

An extra deck driver has been added in order to support a second Loco Positioning UWB deck that can receive UWB inter-agent ranging measurements. The deck driver has support for the wiring diagram as shown in this section. By setting a compile flag, using the modified python Crazyflie Client or crazyflie-suite, the desired UWB algorithm can be selected for every deck individually. The inter-agent ranging algorithm has been inspired on L. Shushuai's github repository on relative-localisation.[3]. Also, the possibility has been added to change the inter-agent ranging algorithms or disable UWB decks in flight by setting the respective parameters.

- **Supporting software developments**

In order to be able to change the settings or command the Crazyflie such that it can perform the desired manoeuvres, both the python crazyflie-suite[4] and Crazyflie client[5] have been used. The crazyflie-suite has been modified to accommodate the needs for this research. This entails the proper trajectory, logging configuration and startup behaviour. The Crazyflie client has been modified in order to support the extra UWB deck. Thanks to this modification, one can view the status or change the algorithm of the individual UWB decks through the client. For an illustration of this modification, please refer to Figure 2.2

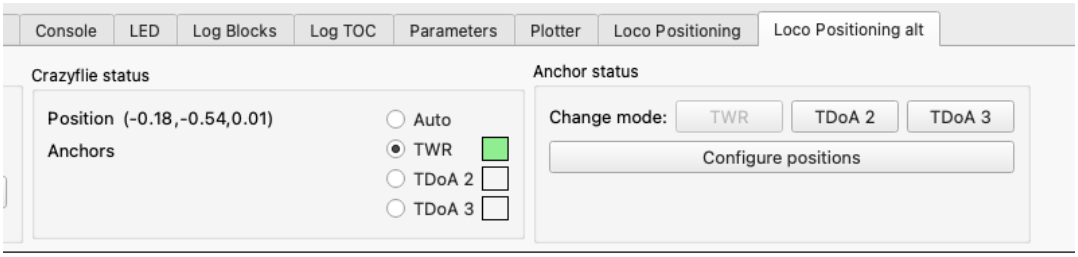

Figure 2.2: Crazyflie client supporting extra UWB deck

- **Crazyflie v2.1 wiring diagram**

The final part that makes this thesis project possible is the modified Crazyflie 2.1. The wiring diagram that makes it possible to accommodate two Loco Positioning System UWB decks and one flowdeck is depicted in Figure 2.3. Please note that due to the fact that the Crazyflie 2.1 only has 4 GPIO pins (which is not enough for the current configuration), the reset pin of UWB deck 2 shares the RX pin used by the Flowdeck v2. It has been found that it is possible to share these pins while giving adequate stability. However, for further developments, it is advised to multiplex one of the four available GPIO pins for expandability and increased stability.

[3] https://github.com/shushuai3/cf_onboard_swarm/tree/swarm
[4] https://github.com/tudelft/crazyflie-suite
[5] https://github.com/bitcraze/crazyflie-clients-python
[6] www.bitcraze.io

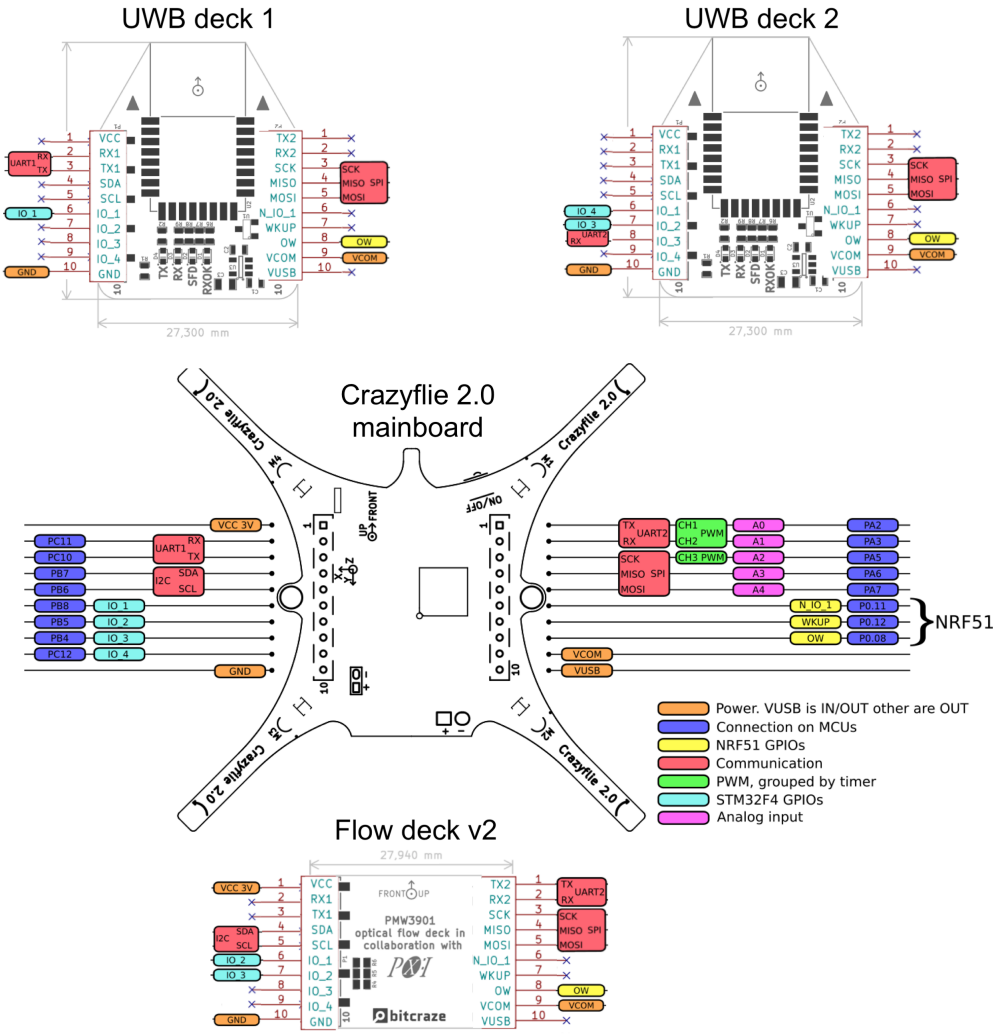

Figure 2.3: Crazyflie 2.1 wiring diagram to accomodate 2 UWB decks and 1 flowdeck v2[6]